

PRE-PHASE A SYSTEM STUDY OF A COMMERCIAL-SCALE SPACE-BASED SOLAR POWER (SBSP) SYSTEM FOR TERRESTRIAL NEEDS

TN4 – APPENDIX 1: SPACE SEGMENT ARCHITECTURE
DEFINITION



REPORT TO
EUROPEAN SPACE AGENCY (ESA)

NOVEMBER 20TH 2023 – REVISION 1.2

ESA Contract No. 4000141171/23/NL/MGu.

**SBSP Space Segment Architecture
 Definition**

[TN4]

SBSP Pre Phase A Study

<i>Written by</i>	<i>Responsibility</i> + handwritten signature if no electronic workflow tool
SBSP Team	
<i>Verified by</i>	
G. Durand	TAS SBSP Study Manager
<i>Approved by</i>	

Approval evidence is kept within the document management system

Change Records

ISSUE	DATE	§ CHANGE RECORDS	AUTHOR
Issue 1	19/10/2023	1st issue for AKR	TAS Team
Issue 2	16/11/2023	2 nd issue post AKR	TAS Team
		-	

Table of contents

1	Introduction	6
1.1	Scope and purpose	6
1.2	Applicable documents	6
1.3	Reference documents	6
2	Reference orbit and constellation definition	7
3	Direct Solar Reflectors design	8
3.1	Platform architecture	8
3.1.1	Structure	10
3.1.2	Reflective membrane	17
3.1.3	Mechanical sizing	18
3.2	AOCS	26
3.2.1	Orbital control	26
3.2.2	Attitude control	27
3.2.3	Pointing accuracy	28
3.2.4	Where size matters	29
3.3	Communication and data handling	29
3.3.1	Communication	29
3.3.2	Data handling	30
3.4	Power	30
4	Budgets	31
4.1	Mass budget	31
4.2	Power budget	32
4.3	Reference architecture synthesis	33
5	Launch and assembly sequence	34
5.1	Launch solution	34
5.2	Assembly sequence	35
6	Safety and end-of-life	40
6.1	Collision risk with debris and micrometeoroids	40
6.2	Collision risk with satellites	47
6.3	Other risks	48
6.3.1	Radiation	48
6.3.2	Space weather events	48
6.4	FDIR and critical events	49
6.5	De-risking approach with demonstration	50
6.6	End of life management	50

7	Technology maturation needs and small scale demonstration	52
8	Annexes.....	54
8.1	DRAMA analysis report	54
8.2	Natural frequencies of the platform.....	54

1 Introduction

1.1 Scope and purpose

This document presents the TAS activities of WP 530 consisting in a support to the architecture description for Space segment.

1.2 Applicable documents

ID	Title	Reference	Issue
[AD1]	ADL Contrat	400011411721/22/NL/MGu/TAS	1

1.3 Reference documents

ID	Title	Reference	Issue
[TN1]	TN1- SBSP System Functional Analysis	0005-0017491435	1
[TN2]	TN2- SBSP Concept Of Operations	0005-0017491451	1
[TN3]	TN3- SBSP Space Segment Architecture	0005-0017491456	1
[NASA]	Conceptual Design Studies for Large Free-Flying Solar-Reflector Spacecraft	NASA-CR-343819810016602	
[Solspace]	A reference architecture for orbiting solar reflectors to enhance terrestrial solar power plant output	Advances in Space Research 72 (2023) 1304–1348	
[ref2]	theory of elastic stability. S.P. Timoshenko. 2 nd ed		
[ref3]	a treatise on mathematical theory of elasticity. A.E.H Love. 4 th ed. 1927		

2 Reference orbit and constellation definition

Thanks to the methodology explained in [TN3], the selected orbit is a 6-18 Local Solar Time (LST) Sun Synchronous Orbit at an altitude of 890 km.

Indeed, the lower the altitude is, the smaller the light spot on ground is and then the necessary number of mirrors to get enough illumination is. It is also beneficial because it minimizes the size of the ground solar installation surface and then reduces the footprint.

Moreover, at this specific altitude, the orbital period is a multiple of 12 hours. The consequence is that each reflector could flyby the same ground site twice a day, respectively at 6h and 18h LST. This is particularly interesting to maximize the use of the same ground sites. However night condition depends on seasonal effects unless for geographic locations of latitudes between $-20^{\circ}/+20^{\circ}$.

On the other hand, a lower orbit brings important shortcomings. First, the increase of drag. Even though still at “high” LEO orbit, given the large and lightweight platform, the effect of the drag is not negligible anymore and would represent an important orbit decay if not compensated by orbit raising manoeuvres as shown in [TN3].

The other shortcoming with lower altitudes is the angular acceleration needed for tracking Ground Power Stations (GPS), i.e. to keep the light spot centred on the GPS while in visibility of it.

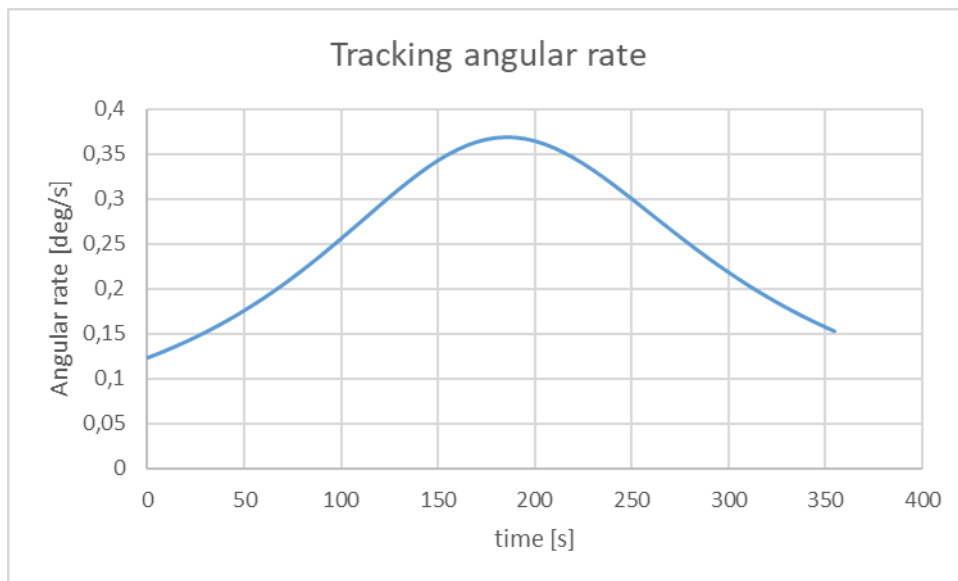


Figure 2-1: Typical angular rates while tracking GPS

At 890 km the max angular rates are typically of about $6.4E-3$ rad/s, implying, an angular acceleration of $2.3E-5$ rad/s².

Moreover, the altitude together with the GPS inter-distance also drives another angular acceleration and max speed to reach. At 890 km and for 4 000 km between two stations, the inter-GPS reorientation implies an angular acceleration of $9.62E-5$ rad/s² and a max angular rate of $1.23E-2$ rad/s for a double sided mirror such as the one considered in this document (to shorten the reorientation duration).

These angular rates and accelerations values will have to be considered for the actuators sizing and the structural constraints.

Once the orbit selected, the number of reflectors can be determined depending on the reflector size and the expected irradiance provided on a GPS. As explained in [TN3], the reflector diameter was set to 1 km. The expected irradiance is of 1 000 W/m². To do so the simultaneous contribution of 257 mirrors equally separated of 12 km along the visibility arc is needed. But because reflectors are on a scrolling orbit, this pattern is only true for a given time and have to be multiplied to extend the GPS illumination up to a given duration. The maximum duration expected to provide light to a given GPS is 2 hours. This implies an "orbital train" of 3 987 reflectors. But because of Earth's rotation, the GPS location will not remain on the 6-18 LST orbit ground track. Consequently, in fact only the first satellite is exactly on a 6-18LST SSO. Each following satellite has a small (7.5 mdeg) increment of right ascension of the ascending node in order to have its ground track aligned with GPS site. It means that the last satellite of the constellation will flyby the GPS site 2 hours later than the first one. It is no longer on a 6-18 LST but on a 8-20 LST SSO. It is important to notice that it was then verified that at 890 km of altitude this last satellite is not yet in eclipse. It was confirmed but 2 hours duration is clearly the limit. Here again, a lower orbit altitude would not have allowed such an illumination duration.

3 Direct Solar Reflectors design

The DSR elements shall be, as much as possible conceived to be disassembled and manipulated by a robotic arm for maintenance and end of life dismantling purpose.

3.1 Platform architecture

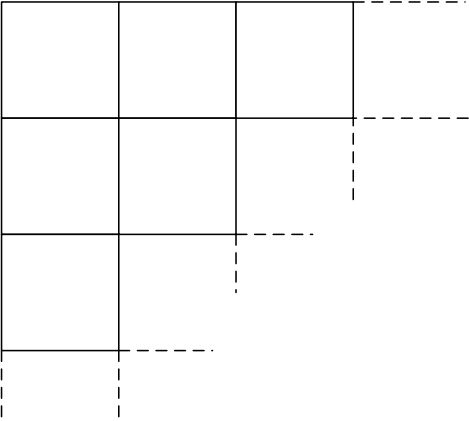
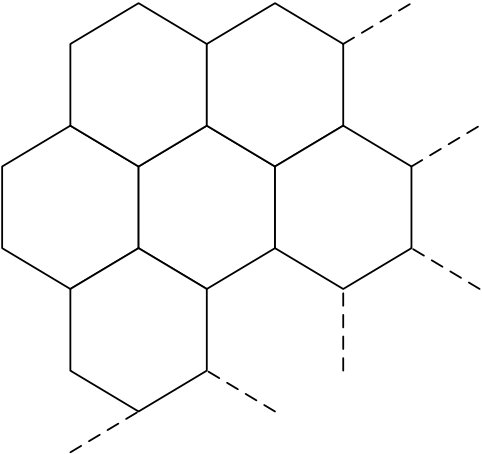
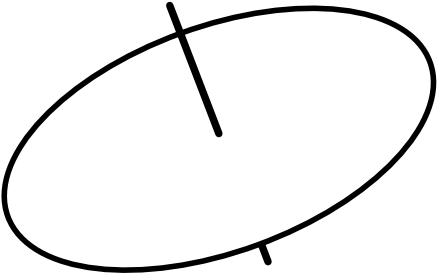
A major point of solar reflector performance is the flatness of the reflecting membrane. To ensure this flatness, the membrane must be sufficiently taut and the structure must maintain its geometry.

To ensure the reflecting membrane tension, a "spring" system must be installed all around the membrane to ensure force distribution (avoid having too large local forces) and avoid folds on the membrane. These tension systems must compensate a thermal expansion of the membrane. The implementation of a membrane tension system has a mechanical impact on the structure into mass and directs the chosen solutions.

To maintain its geometry, the structure must have the greatest possible stiffness. On an object like the plan solar reflector (2 dimensions), it's difficult. To gain stiffness, the structure will have to distribute the forces outside reflector plane. This will impact mass and implementation.

The objective of this study (given the size of the object) is to make a reflector and a structure as light as possible. The inertias for the AOCS must be as low as possible. The reflector choice with the lower thickness and the lower density is necessary. This material must be the most reflective and must be able to unfold in space to take up as little space as possible upon launch. The choice of solid mirror was therefore excluded from the start of this study

For the overall architecture, three solutions were considered with the advantage and disadvantage detailed in the following table:

Solution	Advantage	Disadvantage
<p>Square solution</p> 	<p>Easier solution to achieve individually, then duplicate to assemble in orbit.</p> <p>Ease of deploying the reflective surface (rectangular strips).</p> <p>Allows you to create a small-scale demonstrator.</p>	<p>Lots of structural assembly.</p> <p>High mass</p> <p>Many elements to constitute the objective surface area of 785,000m² (area of 1km of diameter circle)</p>
<p>Hexagonal solution</p> 	<p>Easy solution to make individually.</p> <p>Allows you to create a small-scale demonstrator.</p>	<p>Reflective surface in the form of a triangular element (deployment more difficult than the previous solution rectangular)</p> <p>Lots of structural assembly.</p> <p>High mass</p> <p>Lots of subassembly to constitute the objective surface area of 785,000m² (area of 1km of diameter circle)</p>
<p>Circular solution (base on NASA study NASA-CR-343819810016602)</p> 	<p>Less structure to constitute the objective surface area of 785,000m²</p> <ul style="list-style-type: none"> - Lower overall mass. - Reduced overall inertia. 	<p>Deployment in space (Single launch solution with global deployment or assembly in orbit with multi launch)</p> <p>Deployment of the reflective surface more difficult due to the surface.</p>

3.1.1 Structure

The solution chosen for the study was the circular one with central mast and shrouds. The objective being to move towards a solution with the least structural element to achieve the objective surface area of 785,000m² (launch number reduction, less inertia for the SCAO sub-system). The figure below shows the overall architecture and dimensions.

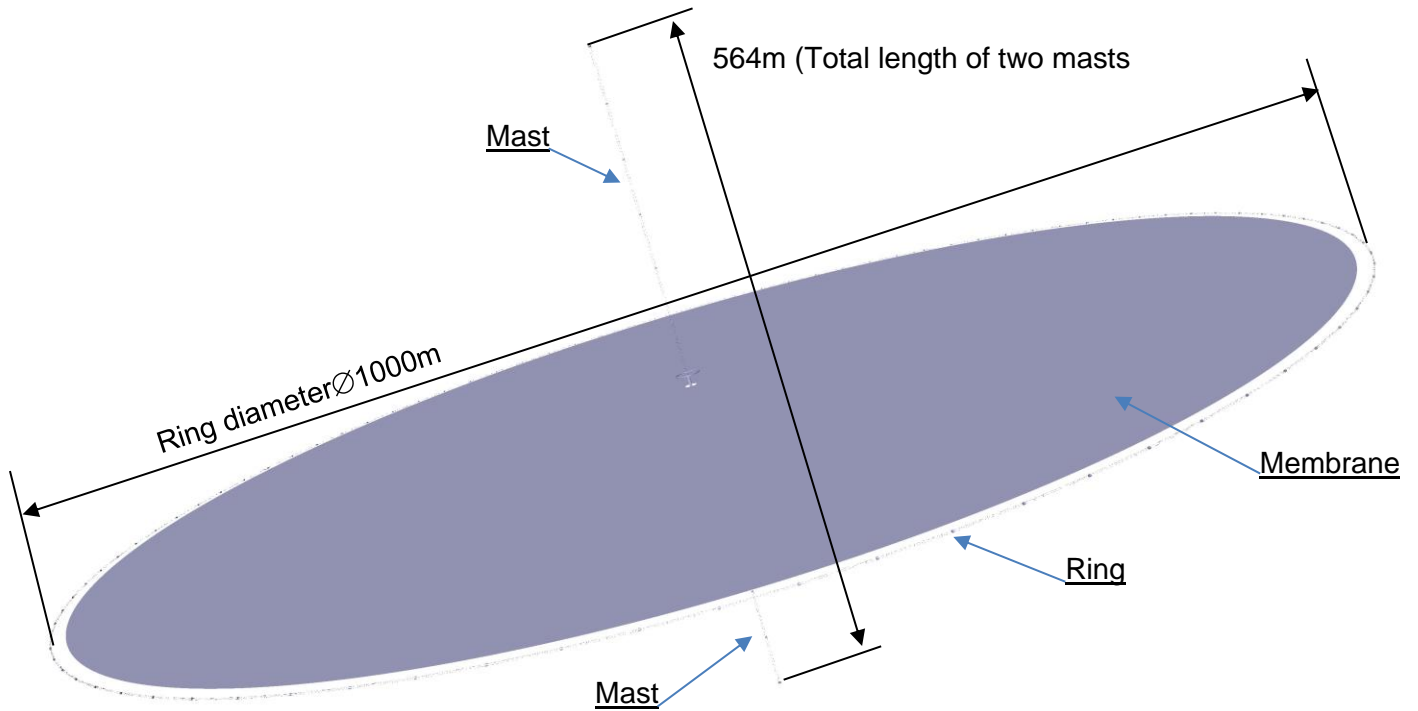


Figure 3-1 : Global view

The ring is made up of 90 compartments including 30 elementary trusses. The following three views show a deployed compartment, the stored compartment and the dimensions of an elementary trusses used for ring.

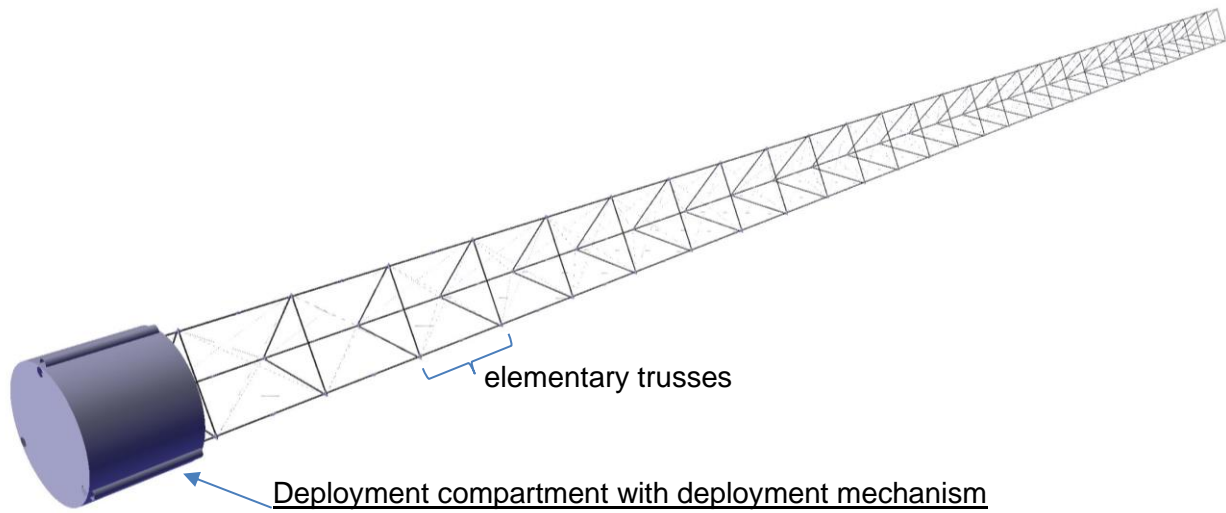


Figure 3-2 : Ring compartment deployed

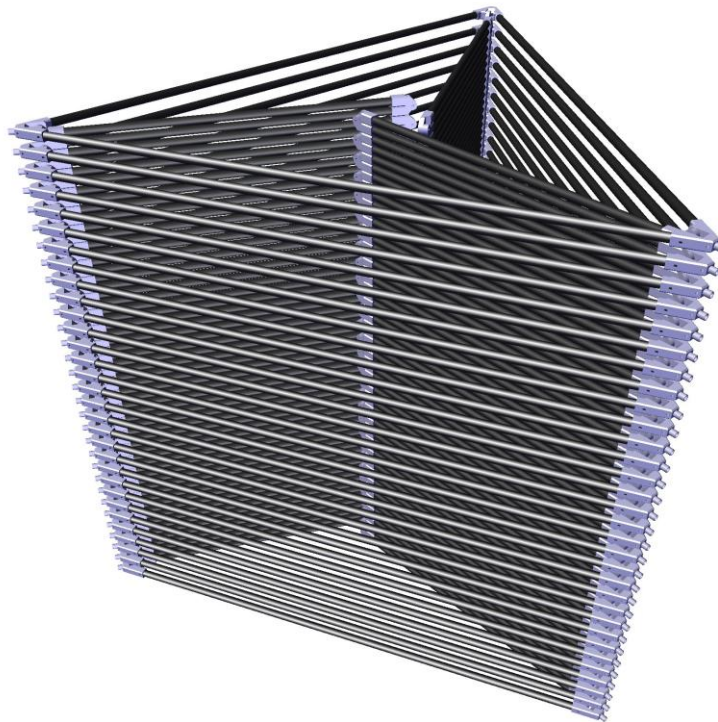


Figure 3-3 : Ring compartment stored

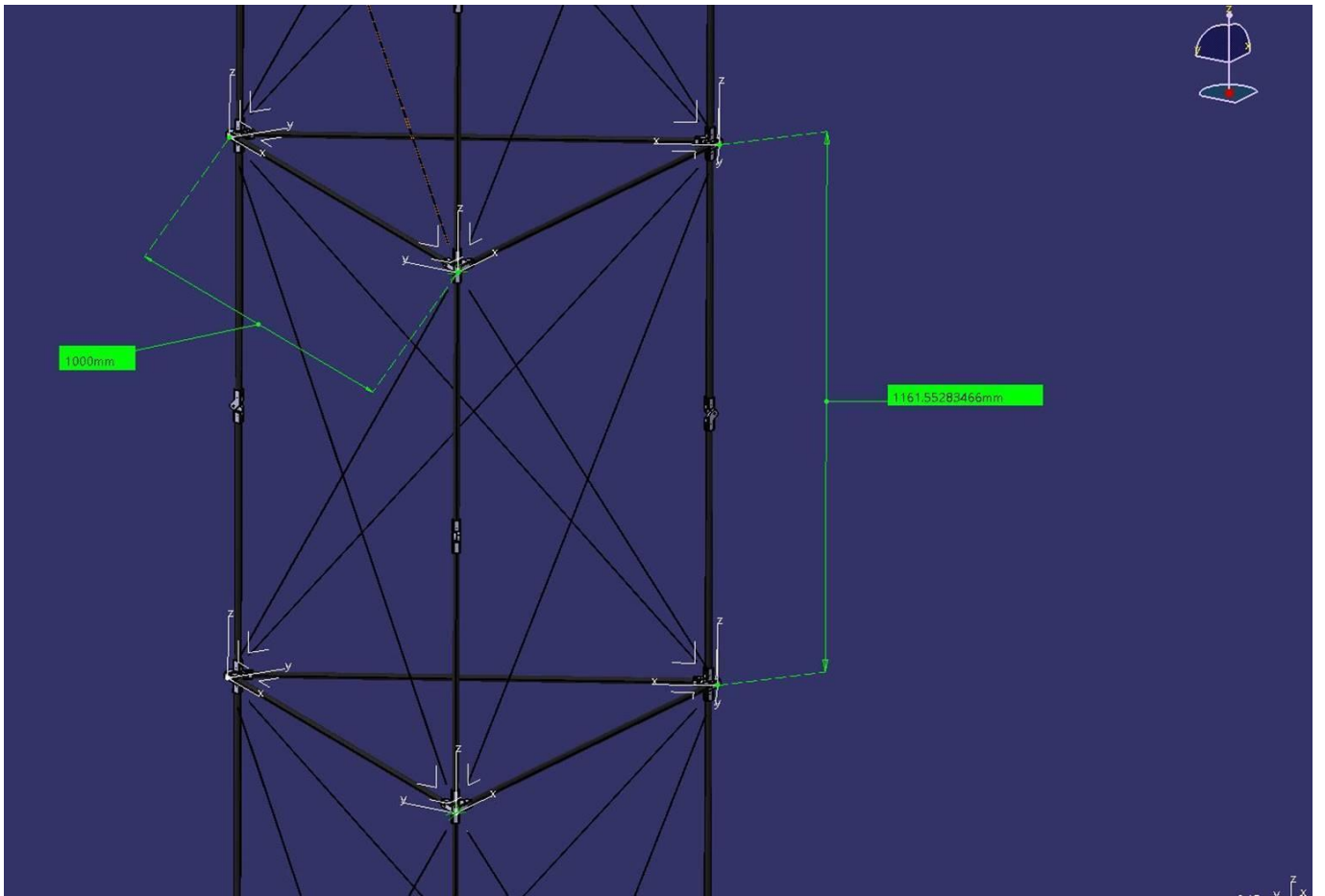


Figure 3-4 : Ring elementary trusses

Each mast is made up of 6 compartments including 30 elementary trusses. The following three views show a deployed compartment, the stored compartment and the dimensions of an elementary trusses used for ring.

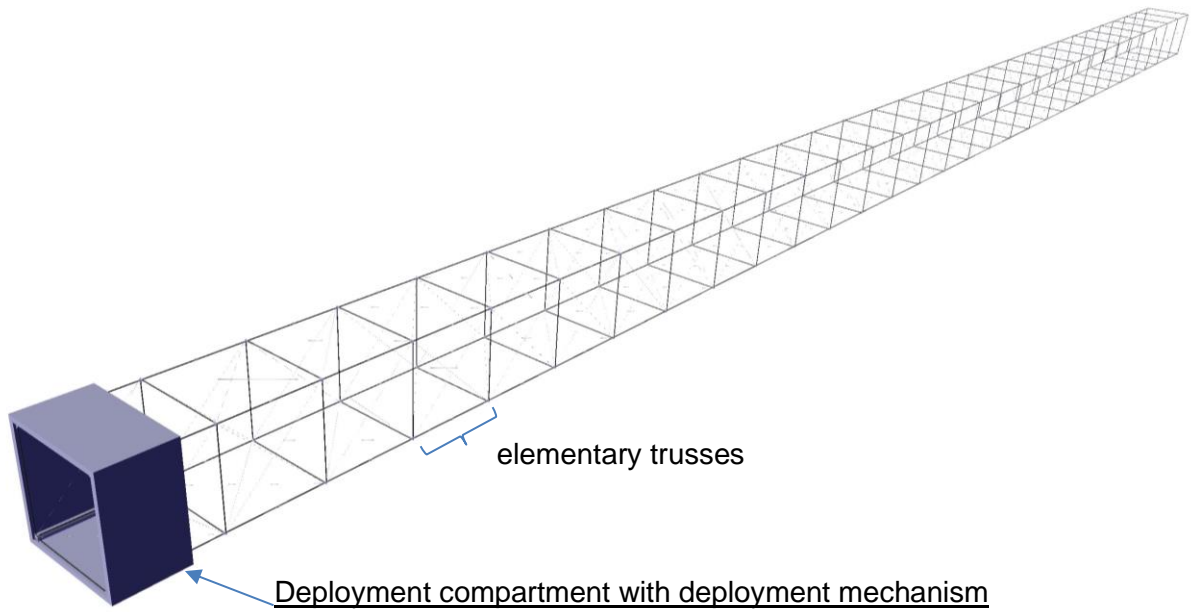


Figure 3-5 : Mast compartment deployed

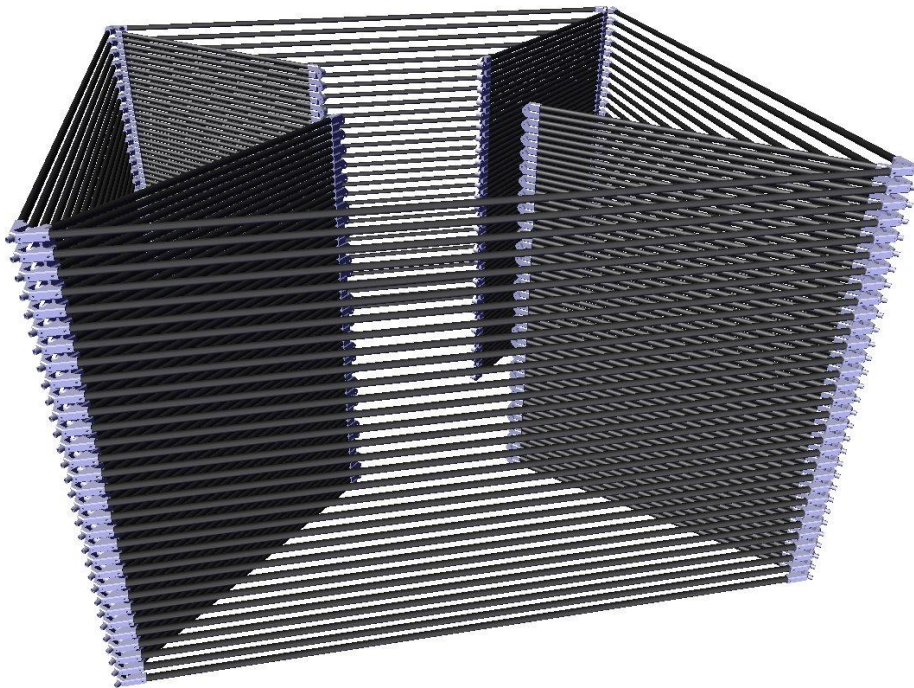


Figure 3-6 : Mast compartment stored

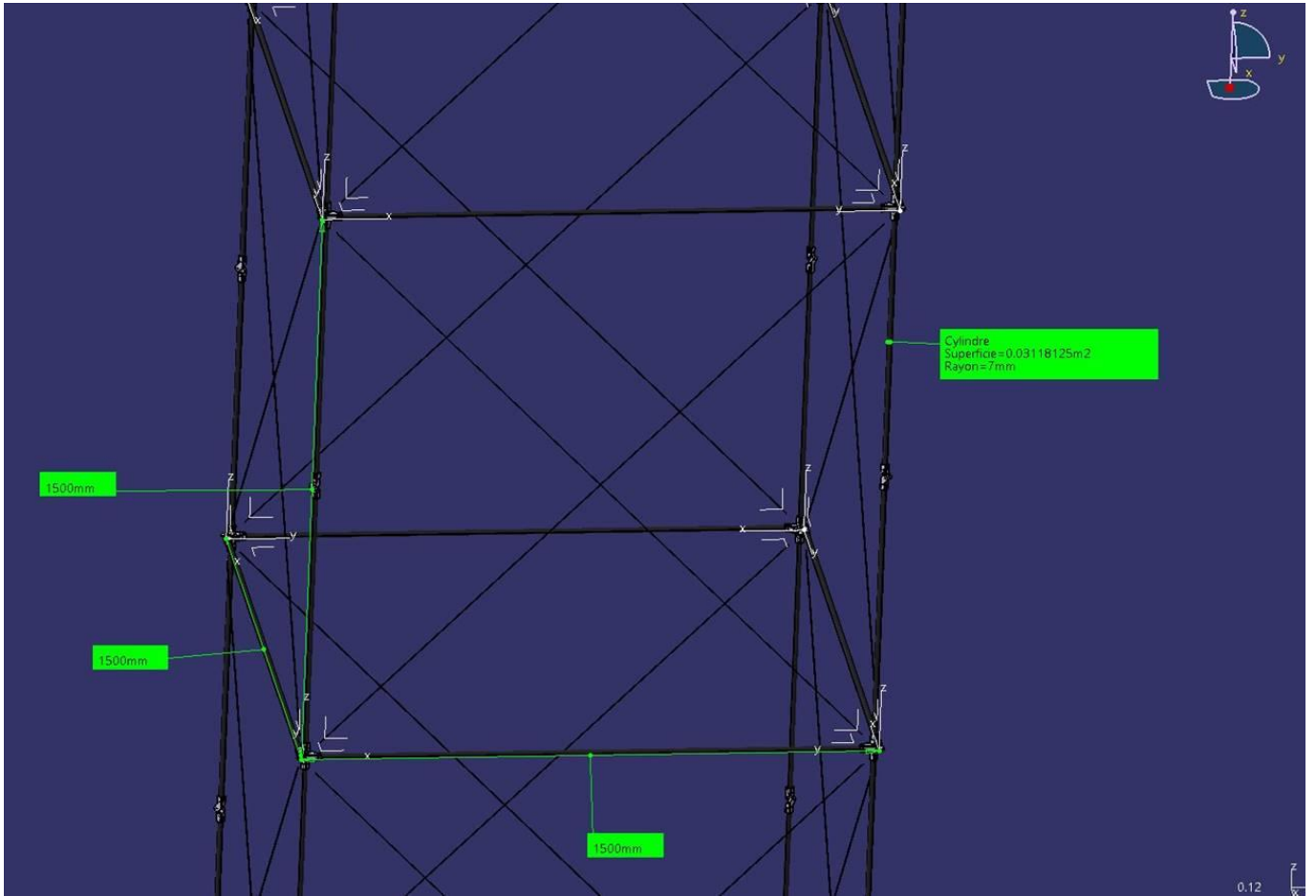


Figure 3-7 : Mast elementary trusses

90 film expansion compensator are fixed on the trusses compartment of the ring and serve to tension the membrane and compensate for its thermal expansion.

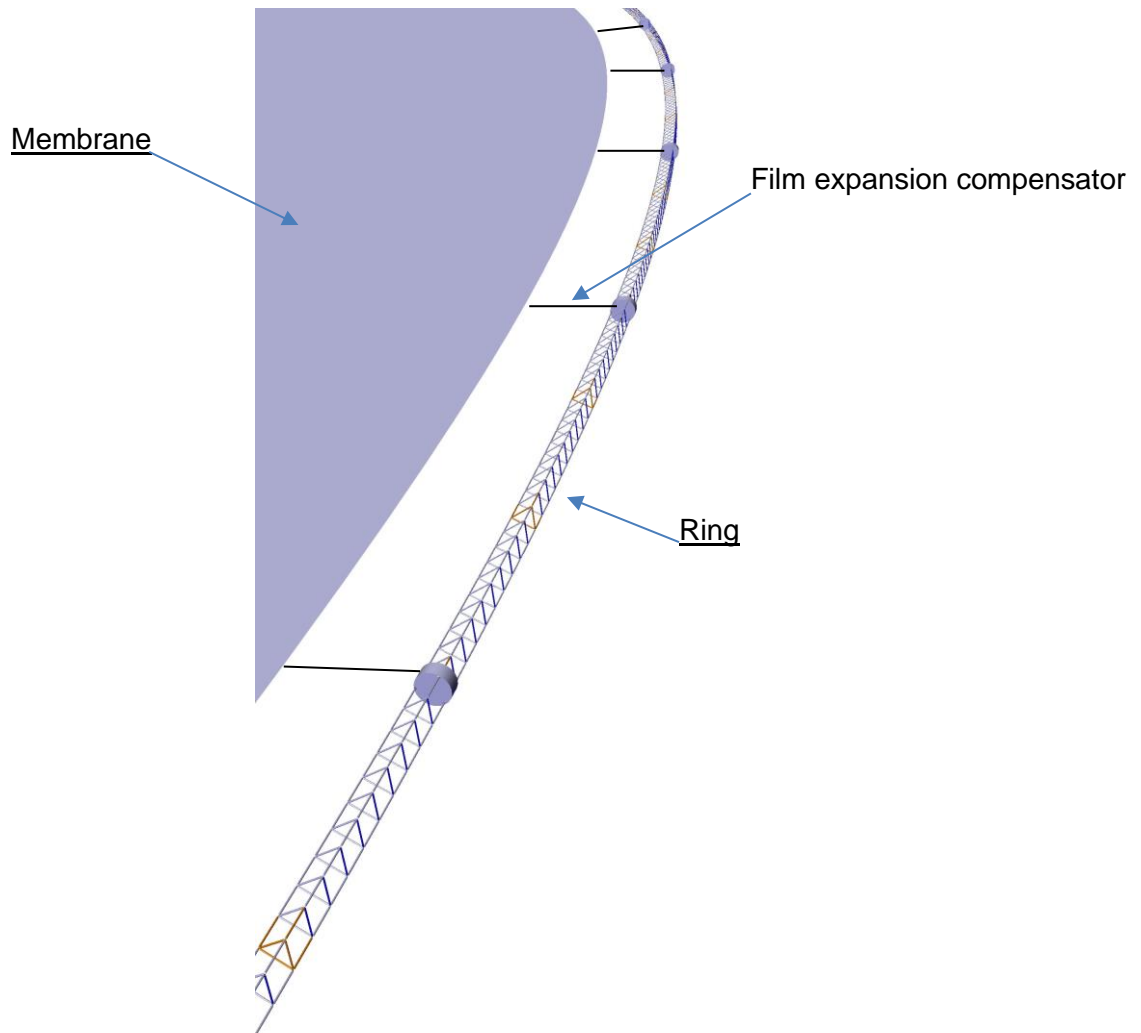
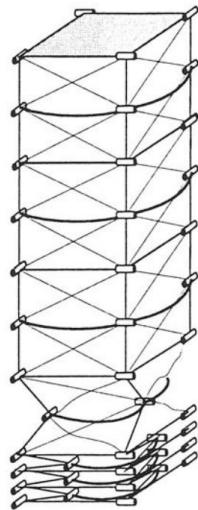
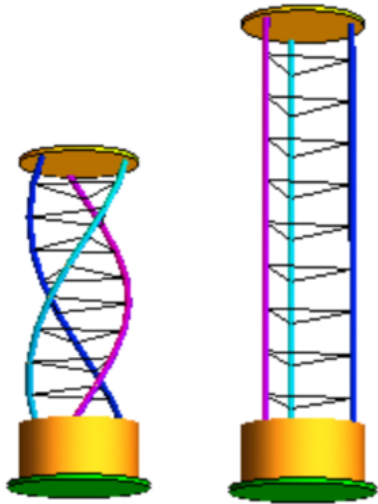


Figure 3-8 : Film expansion compensator

The main part of structure is composed of truss structure (external ring and central masts). These truss structure deploy into orbit. Two technologies were selected for the study. Collapsible truss structure or coilable truss structure. See following table.

	Collapsible truss	Coilable truss
		
Advantage	<p>This box-truss design has been used extensively in other designs of similar systems. The simple collapsing box is easy to understand, analyse, and fabricate</p> <p>This design only has one class of moving part, a spring loaded hinge.</p> <p>These hinges produce the only motion needed for boom extension.</p> <p>Better resistance to compression of the coilable truss structure solution. See § 3.1.3 mechanical sizing</p>	<p>The low mass and small stowage size of this design can allow for flexibility in design choice for the small connectors and stowage configuration.</p> <p>Deployment can be done using the stored energy of the longerons by springs included in the mechanisms - no motor needed</p> <p>This design has very strong flight heritage and resources are available for design reference</p>
Disadvantage	<p>Mass higher (15 at 20% more than Coilable truss solution)</p> <p>Stored dimension higher than the coilable truss structure solution.</p> <p>With a lot of pieces, there is a higher chance for individual part failure.</p>	<p>Stowage of the diagonals may be difficult to accurately predict with each redeployment</p> <p>Very low resistance to compression.</p>

For the solution chosen three major points are to be consolidated by design, analyzes and possible demonstrator.

1) The choice of the reflector membrane.

To gain mass and consolidate the hypotheses:

- Contact the manufacturers to get their opinion on the development of thicknesses thinner than those on the market, objective 4µm max.
- Characterize the mechanical strength of this type of sheet
- Characterize their thermo optical properties
- Sheet deployment and tension model

2) truss structure :

- Even if the deployment trellis system seems to best resist compression, which is the major mechanical constraint of the circular reflector, carry out a design and mechanical analyzes of each of the solutions to have the best mass to size ratio.

Few large bar trellis systems (necessary for the reflector) have been developed (length of 30 to 40m); a demonstrator would be a plus to validate the solution adopted following the design.

3) Membrane tension system:

- Developed a system to have constant tension despite large expansion distances.

3.1.2 Reflective membrane

Two materials were selected for the production of the reflective membrane. PEEK or KAPTON. Both used by Thales for satellite isolation and having a strong heritage and flight. Information on these materials is presented in the following table:

	Unit	PEEK			Kapton		
Material		PEEK™ Aptiv™ polymer films			Kapton		
Manufacturer		VICTREX®			DUPONT / MICEL		
Thickness	µm	4 (hypothesis)	8	25	4 (hypothesis)	7,5	25
Development maturity	TRL	Not yet produced	9	9	Not yet produced	9	9
Density	kg/m3	1300			1420		
Mass	g/m²	≈ 6	10.4	32.5	≈ 7	10.6	35.5
Coefficient of Linear Thermal Expansion	ppm/°C	47			46		

Fracture strain	%	>150			72		
Moisture absorption 23°C, 24h, 50%RH	%	0,04			18		
Cost	k€/kg		0.42	0.26		1.3	0.55
Qualification temperature	°C	-180 / +250			-180 / +250		

The baseline for future studies will be PEEK because it has better tear resistance, lower density (mass) and is ITAR free. The cost of PEEK material is around a half of Kapton.

Two types of leaves were analyzed. aluminized 1 or 2 sides.

The table below gives the temperature reached by the membrane for the two cases depending on the flight attitudes.

Membrane temperature	Aluminum one side	Aluminum two sides
Nominal mode	-26°C	+173
Fully sunshine (sun normal to reflector)	+3°C	+183°C
Eclipse	-103°C	+8°C

The temperatures are compliant to qualification of materials

The maximum expansion relative to 20°C of 2 sides aluminized PEEK is as follows:

-0.6m when the reflector is at +8°C in eclipse

+7.5m when the reflector is at 183°C in fully sunshine

Maximal 10m is a good values to be considered for the next studies.

This value will be taken into account for the design of the tensioner and the structure.

The two products are compatible, the choice will be made according to the mass and discussions with the manufacturers for thinner thicknesses. But the PEEK material is considered for a baseline for this study.

3.1.3 Mechanical sizing

3.1.3.1 Introduction

This paragraph provides the sizing elements and computations which support the design of the rim truss and of the principal mast(s).

For accommodation considerations in stowed configuration it is selected:

- For the rim-truss
 - a triangular cross-section for the rim-truss in “astromast-like” concept,

- a square section for the rim-truss in “hinged-mast” concept;
- For central mast, a squared cross section is preferred.

A leading consideration is to insure the flatness of the mirror in mission, so that the reflected solar beam flux do not diverge, while the mirror is under solar pressure. This fixes for a sufficient tension in the supporting elements, which results in compressive effort in trusses (rim and central-masts), and lead to size the beams-truss in compressive axial buckling.

Two configurations are evaluated for the deployable elements (rim-truss and the deployable central masts), and briefly stated, as supporting by the follow of the present paragraph, the conclusion comes as follows:

3.1.3.1.1 Summary of the conclusion

“Astromast-like” solution:

- The concept does not appears to comply easily both the necessity of
 - a sufficient axial buckling limit load AND
 - easy accommodation in helix stowed configuration.

A preliminary computation allows to evaluate a possible solution (based on an imposed axial torque, along the axis of the helix in stowed configuration) but the solution is sensitive to value of this torque, and small relative discrepancy will result in (too) large compressive forces (along helix axis).

It looks to us that this solution is more adapted to missions where limited axial buckling is required.

“hinged-mast” solution:

- The concept accepts easily to comply a sufficient bukling rigidity (in deployed configuration) AND
 - a limited value of the efforts in stowed configuration.
 - No strong dependence of stowed configuration geometry with accuracy onto the stowing efforts.

The solution depends onto good manufacture of the hinge, for which reasonable confidence can be foreseen.

We detailed now the sizing computation which leads to the precedent conclusion.

3.1.3.2 General considerations

The following assumptions are considered in input

Rim truss diameter	[km]	1
Principal mast height above the mirror	[m]	270

Rim truss : rational for the sizing.

The rim supports the mirror in deployed configuration, where the geometry of the plane mirror is challenged by the following constraints:

Constraint		Details and values	Comments and Origin of input.
flatness in quiet configuration	N° 1	<p>The rim supports the radial load resulting from the solar pressure onto the mirror.</p> <p>The maximum solar pressure onto the mirror of radius r is:</p> $P_0 = 2 \pi r^2 = 7.11 \text{ [N]}$ <p>Which is estimated from the solar pressure of a perfectly reflecting surface; with normal at angle γ from incident solar flux:</p> $0.9 \text{ E-5 } \cos^2(\gamma) \text{ [N / m}^2 \text{]}$ <p>Under this flux; a maximum flatness deviation evaluated as a spherical deformation of the mirror result in a 18% loss of flux for an edge gradient of 0.001 [rad] (from NASA); Considering the here-above 1E-5 [N/m²] maximum solar pressure, the membrane required tension is evaluated at</p> $T = 1.25 \text{ [N/m].(from } \text{[NASA], fig 17)}$ <p>The total compressive load on a truss segment induced by this radial tension, distributed by n_0 tendons equally spaced is</p> $B = \sin[\pi / 2 (1 + 1/n_0)] / \sin(\pi/2 1/n_0) = 28.63$ <p>for n_0 at 45 (on a half rim length).</p> <p>Onto the total length of a truss segment L,</p> $L = 35 \text{ m}$ <p>the tension is T L , and the compressive load</p> $P1 = T L B \text{ [N];}$ <p>It results $P1 = 1252 \text{ [N]}$</p> <p>This is assumed 2/3 of total compressive load, while 1/3 additional is induced by the links to central mast tension , resulting in a total P [N] compression in the truss.</p> $P = 1875 \text{ [N]}$	<p>From [ref 1].</p> <p>In fig17 NASA we read a slightly higher value, closer to 2</p> <p>We retain this 1875[N] of compression as our sizing input (note that this is also the value of NASA)</p>
Impact of maneuvers; angular accelerations.	N°2	<p>The mirror is pointing the solar-farm on earth, while orbiting at 890 km;</p> <p>The resultant angular accelerations are evaluated at</p> $2.3 \text{ E-5 [rad sec}^{-2}\text{].}$	<p>See §3.2.2.1</p>

	<p>The mirror performs re-pointing, from one earth solar-farm to the next. Considering 4000 km inter-far distance, the accelerations is evaluated at</p> <p style="text-align: center;">9. E-5 [rad sec⁻²]</p>	<p>We compute a preliminary impact of the maneuvers, as resulting from a sizing imposed by constraint n°1</p>
--	---	---

The rim-truss in stowed configuration imposed a limited external diameter of the longeron rod. After discussions with mechanical architect, a value of 14 [mm] is selected. Mass consideration impose to limit the internal diameter, a 12 [mm] is selected (for carbon fiber rod).

$$.r_{ext} = 7. E-3 [m]$$

$$.r_{int} = 6. E-3 [m]$$

The bukling critical load is estimated form Euler bukling

$$P_c = \pi^2 E I_s / l_o^2$$

Where l_o the length of a longeron is taken at

$$l_o = 1.16 [m]$$

considering a carbon rod we consider

$$E = 200 E9 Pa$$

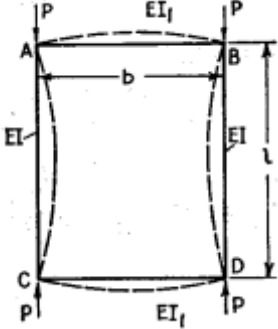
The quadratic area momentum (surfacic inertia), I_s , will results from the internal diameter r_i

$$I_s = \pi (r_e^4 - r_i^4) / 4 = 8.68 E-10 [m^2]$$

And the critical load (in 1 longeron)

$$\mathbf{P_c = 1270 [N]}$$

The resistance to buckling is enhanced by the transvers rod; a rapid first estimate of the enhanced stiffness can be proposed considering transverse rods of equal material section and length than the longeron and joints between longeron and transverse perfectly rigid, in case of symmetric buckling in the plane, it results:

<p>Symmetrical buckling of the cell:</p>		<p>From [ref2]</p> $P_{c1} = 1.67 P_{c0}, P_{c0} = 1.67 \pi^2 E I_s / l_0^2$ $P_{c1} = 2109 \text{ [N]}$
--	---	--

A more elaborated compute should takes into account the two transverses in A (at 60° angle), and buckling along the bisector of transverse. In time available, we propose this P_{c1} value.

The load in the longeron is hardly the total 1875 [N] load, as this one is distributed onto the 3 longerons; when considering $1875 / 3 = 625 \text{ [N]}$. the margin to P_{c1} is to be more evaluated; for our preliminary present sizing we propose the present definition.

Note that with this section and modulus E of longeron, the relative compression under 625 [N] is

$$d_l / l_0 = 7.6 E^{-5}$$

Which confirms that constraint is far from limit.

The global buckling of the column (cylindrical of 35 m of triangular section with longerons rod at each summit of the section) can be estimated while considering a radius of 0.5 m; which put a Euler 1srt buckling load far above P_{c1} (a factor 10 higher than P_{c1}).

3.1.3.2.1 Stowed “astromast-like”.

The 35 m column of 3 longerons lines is assumed stowed as an helix. We consider first one helix of 1 rod of 30 longerons length.

From [ref3] § 270;

R is the axial effort at both end of the helix. (R negative is compression); R_0 the radius of helix; K the axial torque at both end of helix. $\psi \theta \phi$; the euler angle, t the twist of the rod, s the curvilinear coordinate along the rod; α the helix angle. (angle between tangent to the rod and the plane orthogonal to helix axis).

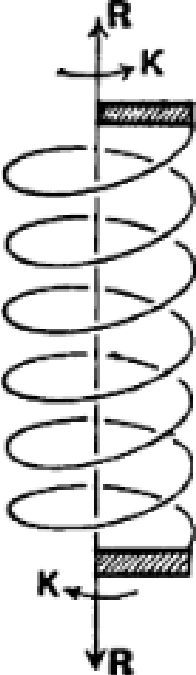
In a completely stowed configuration at compact spiral (rod in contact); the α angle is

$$\alpha = 2 r / (2 \pi R_0)$$

(in our case, considering a 2 r value at 14 [mm] and a helix radius at 0.5 [m]; it will results

$$\alpha = 4.45 \text{ E-3}$$

This value will appear constraining but a α angle results in less compact stowing, and difficulty in total accommodation (under fairing limit ...).

<p>Case of one rod stowed at helix</p>	 <p>The diagram shows a vertical helix rod. At the top end, there is an upward-pointing arrow labeled 'R' and a rightward-pointing arrow labeled 'K'. At the bottom end, there is a downward-pointing arrow labeled 'R' and a leftward-pointing arrow labeled 'K'. The helix is drawn with several loops around a central vertical axis.</p>	<p>From [ref3]. (Same notations as [ref3] except for R_0. Which is noted "r" in [ref3]).</p> <p>End torque and effort at both end of the helix:</p> <p>Axial end effort</p> $R = C \tau \cos(\alpha) / R_0 - B \sin(\alpha) \cos^2(\alpha) / R_0^2$ <p>Axial end torque</p> $K = C \tau \sin(\alpha) + B \cos^3(\alpha) / R_0^2$ <p>B is the transverse stiffness $E I$ of the rod , with I the surfacic inertia of the cross-section, and C the torsion stiffness, $G J$, (we consider here G at $E/2.66$) consider $E/2.66$) and J the polar (surfacic) inertia of rod cross section.</p> <p>In our rod, we find B at 200 and C at 131 [SI].</p> <p>R alone</p> <p>For understanding, consider the case of twist τ which results in <u>zero K, and the helix is maintained by compressive R alone;</u></p> <p>Then</p> $R = B \cos^2(\alpha) / (\sin(\alpha) R_0^2) ; \text{ and } \tau = - B \cos^3(\alpha) / (C \sin(\alpha) R_0) ;$ <p>\Rightarrow The resulting R is several thousand of kilo.</p> <p>K alone</p> <p>So that a solution where <u>axial torque can be injected at both end</u> is much preferable, which results in</p> $K = B \cos(\alpha) / R_0 ; \text{ and } \tau = B \sin(\alpha) \cos(\alpha) / R_0 .$ <p>With the characteristics of the longeron rod exposed at precedent § we find</p>
--	--	---

		<p>⇒ $K = 300$ [N m] and $\tau = 8.8 \text{ E-}3$ [rad/m] (this τ will result in a rod rotation along its centerline of 3.2 deg/turn).</p> <p>The problem can be that a <u>slight deviation</u> of K injected value will rapidly results in a <u>strong (unwanted) axial R</u>.</p> <p>And .. it is now to add the two other rods.</p>
--	--	---

Clearly, our analysis does not consider the distributed impact of local torsional torque (along centerline) which is to be added as due to the effect of folding the transvers rod; nonetheless, we consider that our compute shows that difficulties can be expected in the “astromast-like” solution.

This difficulty results from the constrain to stowed in helix a beam that in our application is required “stiff” in buckling.

3.1.3.2.2 Stowed “hinged-mast”.

No difficulty appears, because all the stowing stiness is independent of the buckling capability of deployed column.

3.1.3.3 Central mast

We propose for the central mast a square cross-section of 1.5[m] side;

$$. \text{lsq} = 1.5 \text{ [m]}$$

The tension in cable is assumed resulting in rim-truss compression 1/3 of the 1875 [N]; which results in compression at top of central mast of

$$P = 1875 \text{ [N]} / 3 / 2 (\sin(\beta) / \cos(\beta)) * 2$$

Where the last factor 2 holds for the 2 assembly of cable (each side of planar mirror); and the angle β is the angle of cable with the plane of the mirror.

$$\text{Tan}(b) = 270\text{[m]} / 500 \text{ [m]}$$

This results in

$$P = 337 \text{ [N]}$$

While the critical buckling load, for a 270*2 [m] is

$$P_c = \pi^2 E I / L^2$$

. Considering identical longerons than for the truss rim. we would got 2 sections each of 4.08 E-5 [m²], at distance d from the square center

$$; d = \text{lsq} \cos(45^\circ) = 1.06 \text{ [m]} ; \text{ with } \text{lsq} = 1.5 \text{ [m]}$$

Resulting in I at 9.2 E-5 [m⁴],

The mast is loaded by transverse effort due to the membrane mirror, which will restrained the buckling at mid mast; we consider nonetheless a total length of 2*270 [m], (not accounting for the restraining condition at mid-mast); and we find

$$P_c = 622 \text{ [N]}.$$

The true critical load will be higher, because we do not include in this computation the additional buckling stiffness due to the transverse; which ensure us that the design is strongly sized.

3.2 AOCS

3.2.1 Orbital control

Orbital control is needed for:

- Orbit raising from the parking orbit where the reflector was assembled up to the final orbit location,
- Orbital station keeping, essentially because of the remaining drag force at 890 km,
- Collision avoidance manoeuvres

As it was shown in the [TN3], the yearly cost to compensate the altitude decay with control jets is huge, even with very efficient electrical propulsion: about 540 kg of Xenon for a single reflector. If multiplied by the number of reflectors composing the constellation, it leads to an unrealistic amount of fuel to be brought in space yearly. A smarter and more viable solution is to take advantage of the extremely large and lightweight surface of the reflector to use it as a solar sail for orbital control. This is also what is proposed in [NASA] and [Solspace] studies.

In [NASA], it is shown that solar sailing from 680 km up to 890 km should take about 50 days. However, starting from lower altitude would increase rapidly the duration due to atmospheric drag.

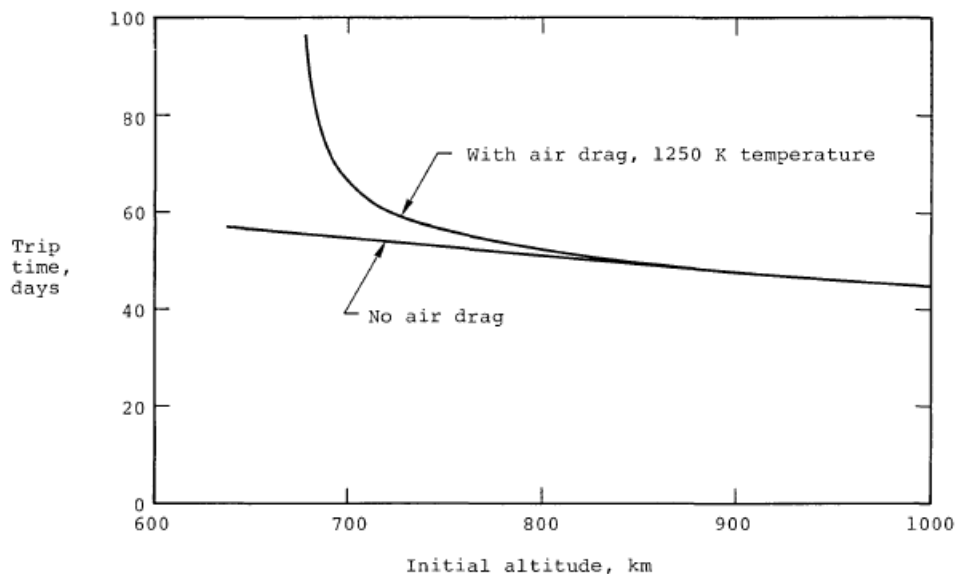


Figure 3-9 : Film Trip time up to 2400 km. Credits NASA [NASA]

Then solar sailing is adequate for orbit raising as long as launcher injection is above 680 km. Nevertheless, it still has to be estimated if with such a method the control authority allows to perform station keeping manoeuvres while solar sail attitude is constrained by direct solar reflection towards ground stations, and also if it is compatible with orbit insertion in the constellation. For this latter case, a solution could be to insert new reflectors at the head or at the tail of the constellation train. Moreover, if deemed necessary, spacetugs could participate to special orbital control manoeuvres.

3.2.2 Attitude control

3.2.2.1 Main actuator

In the part 2 of this document, it was explained that due to the orbit choice and the minimum inter-GPS distance, the following angular accelerations will have to be applied to the platform.

Constraint origin	Max angular acceleration [rad/s ²]	Max angular rate [rad/s]
GPS tracking	2,32E-05	6,44E-03
Inter-GPS repointing	9,63E-05	1,23E-02

Angular rate and accelerations

Among these two, the inter-GPS acceleration with double sided reflecting membrane is the most demanding with 9.63E-5 rad/s². This is the value to be considered for the attitude control sizing. Note that inter-GPS slews are always performed through a straight path to minimize the slew duration, since there is no exclusion constraint because a single reflector irradiance contribution is very small.

The peripheral acceleration at the maximum rotation rate is limited to 7.5E-2 m/s² which is not considered as stressing for the structure.

Since the inertia about the platform diameter is 4,91E+08 kg.m², the necessary torque to be applied to reach this angular acceleration is 47 262 N.m, which is huge with respect to the largest existing CMG in space, which are used in the ISS and can provide a torque of 258 Nm.

For a preliminary sizing, one can consider that the torque T of the CMG is proportional to product of the angular momentum of the wheels H_w with the gimbals angular velocities $\dot{\theta}$.

$$H_w \times \dot{\theta} \cong T$$

Where $H_w = I \times \omega_w$ where the inertia about the diameter is $I = \frac{1}{2}mr^2$ if we approximate the CMG flywheel rotor as a thin rotating ring of a mass m and a radius r .

Then one can notice that the main driver of the torque of the CMG is the radius of its flywheel as it weights to the square with respect to other parameters of the above equation. This is why it is highly preferable to favour very large but lightweight flywheels.

Then, to reach the needed torque for manoeuvring, the sizing led to two two-axis CMGs mounted one on each side of the central part of the mast, one on each side of the mirror membrane. Flywheels axis are aligned with the central mast axis. But since these flywheels have to be extremely large, their sizing have to limit the tilting angle.

Each flywheel has a diameter of 20 m, a mass of 650 kg, providing an inertia of 32 500 kg.m², spinning at 1500 roll per minute. These flywheels actuated by gimbals are able to tilt them at an angular rate of 4.6E-3 rad/s which is low in order to limit the needed tilt angle and also to prevent from gimbal lock effect.

In order to resist to the important centrifugal acceleration of 246 740 m/s², the flywheel could be a rigid rod of 650 kg made of carbon-resin with a density of 1600 kg/m³, and if so it would have a cylindrical section of 9 cm.

Of course elements (bows and radiuses) of these two 20 m diameter flywheels should be assembled and/or deployed once in orbit in order to fit into the launcher's fairing.

One can notice that with such an attitude control system, there is no control about the reflector axis with the CMG. This is correct if we only consider the gimbals action, but changing the flywheels rotation speeds provide an additional (third) degree of freedom about the reflector axis which is anyway not meant to be solicited.

At first order, it was estimated that the average power consumption needed for the attitude control with two CMGs is about 200 W with peak power need estimated to about 600W to reach the max inter-GPS torque of 47 kN.m.

Remarks:

- There is no redundancy of the two CMGs themselves, but their constituting elements could be redounded (gimbal, motors,...). They shall be design to prevent any failure (Single Point of Failure). Moreover in addition to the redundancy integrated into the CMG, there is also a structural redundancy in the mirrors: if one of the 3,987 mirrors is impacted, the others can function while the repair is being carried out.
- With no particular flywheel failure, there is no vibration on the supporting structure, the flywheel can be perfectly balanced (static and dynamic) after assembly and during lifetime thanks to maintenance robots.

If there is a failure in the mechanism supporting the flywheel while the flywheel is parallel to the mirror, the membrane is spared. A contra-rotative wheel break-up could lead to SPS destruction in the worse case.

3.2.2.2 Secondary actuator

In order to desaturate the CMGs, and also to participate to the attitude control, it is also foreseen to use a secondary actuator.

3.2.3 Pointing accuracy

Even if for this preliminary AOCS sizing the large platform was considered as rigid, it should in reality be considered as flexible, with main modes estimation provided in annexe 2 (ranging from 0.025 to 0.25 Hz according [NASA]). To deal with this flexible platform while keeping an accurate pointing necessitates to employ an accurate positional reference system.

The need is to avoid beam excursions beyond about 2.5% of the spot size, which represent approximately 225 m. This implies a pointing accuracy of 0.25 mrad to be performed.

To do so, two actuators are involved:

1. The platform attitude control itself, relying on CMGs and dynamic balancing,
2. The mirror shape, thanks to tendons connected to the membrane on one end, and to the spokes on the other end, ensuring a dynamic shaping of the membrane

The control loop will have to deal with low frequencies. This loop will rely on various real time sensors: star trackers, Inertial Measurement Units (IMU), cameras, strain and temperature gauges, laser telemetry, ... dispatched onto the platform to ensure the pointing accuracy.

Moreover: in order to feed the closed loop controller, it is proposed to use the sensing method inspired by large antennas pointing. The RF sensing method consists in a combination of RF measurements via the RF sensing system. RF measurements are performed through quartets of dedicated beams placed on the platform, centred on a number of fixed ground beacons. The pointing errors are derived from on-ground processing of those measurements, and a corrected set of actuators commands is regularly computed and uploaded to the satellite to compensate the errors.

3.2.4 Where size matters

The description of the AOCS part and the challenges it has to deal with raises questions about the choice for large diameter reflectors, and one can object that probably a smaller diameter could be wiser. So let recall the reasons which led to select a 1 km diameter listing the advantages and drawbacks.

Advantages:

- Mass and cost optimization thanks to scale effect. Indeed, many heavy and costly elements hosted on the reflector do not scale up when increasing the structure size (e.g. computer, interfaces, ...). This is also true for the operations. This is why it is preferable to size the platform up to the limit of today known technical feasibility.
- Large diameter give more distance between reflectors: 14.3 km for 1 km diam. reflectors, 3.5 km for 0.5 km diam. and 0.9 km for 0.25 km diam. reflectors. Lower diameters can even lead to "contact" between reflectors.
- Large diameter induce less reflectors: 3 987 for 1 km diam., 16 000 for 0.5 km diam. and 64 000 reflectors for 0.25 km diam. A large number of reflectors implies more operational costs, more unitary elements, ...

Drawbacks:

- More difficult attitude control. As shown in this part and in annexe 2, large structure implies greater inertias and more flexible modes to deal with, implying a leading edge AOCS solution while smaller diameters would raise less difficulties and potentially allow to adopt existing solutions.

3.3 Communication and data handling

3.3.1 Communication

The communication between ground and reflector is limited to housekeeping telemetry to report the reflector status, and AOCS parameters. If need be, some sensors data could be downloaded for monitoring or investigations. Evenly, limited telecommands should be sent by the ground control centre, essentially to plan attitude and manoeuvre plans.

Consequently, given the low altitude orbit, a simple S-band communication subsystem with a few kbps of TMTC and two omnidirectional small antennas (less than 1 kg each) should be sufficient to cover the mission's needs. In addition this equipment is very resistant to the space environment (some of them were used on Rosetta mission) and transceiver only require about 5 W to work, for a mass of about 5 kg.

3.3.2 Data handling

The computational need is very limited for reflectors normal work, as it essentially loads and propagate orbits and applies the manoeuvring plan. However, in some critical situations like after a collision with a debris, the reflector should be able to manage safety attitude or orbital manoeuvres autonomously and to do so to be able to elaborate quickly a status of the situation by processing information from several sensors. Moreover the constrains of reliability and life expectancy in space environment are of course also critical. This is why we can consider to use data handling subsystem similar to existing ones for small generic platforms, including their on-board computers with an additional redundancy and hardening to comply with the mission. Then a power consumption of 30 W and a mass of 10 kg can be considered. Two units are required for redundancy purpose but only one is used at a time.

A set of AOCS sensors are needed. It is composed of two sets (for redundancy) of: 3 star trackers, 2 Inertial Measurement Units (IMU). Each set mass is estimated to 10 kg. The pointing accuracy could also be ensured by a closed loop with ground sensors feeding the control loop through communication subsystem.

A set of monitoring sensors like cameras, strain and temperature gauges, are also dispatched on the structure. These are low consumption sensors, using Internet of the Things technologies. It is assumed they represent a mass of 30 kg and a power consumption of 30 W.

3.4 Power

The power subsystem is in charge of power generation, storage and dispatching in order to feed the electrical equipment of the reflector of which the average consumption is estimated to 283 W. To do so, the power subsystem is composed of:

- Solar generators accommodated on the tips cylinders of the upper and lower masts in order to see the Sunlight when tracking or repointing the GPS. A total surface of 70 m² was estimated to wrap these cylinders, leading to a mass of 255 kg.
- Batteries, to store energy of exceeding power collected from Sun during daylight and providing power while in eclipse. A total mass of 15 kg of batteries (typically composed of SAFT Li-ion VES16 elements) was provisioned to cover the energy storage need of 30 years.
- Power management: necessary elements to transform and supply power to the demanding elements. These elements overall mass is estimated to 30 kg (they are doubled for redundancy).

4 Budgets

4.1 Mass budget

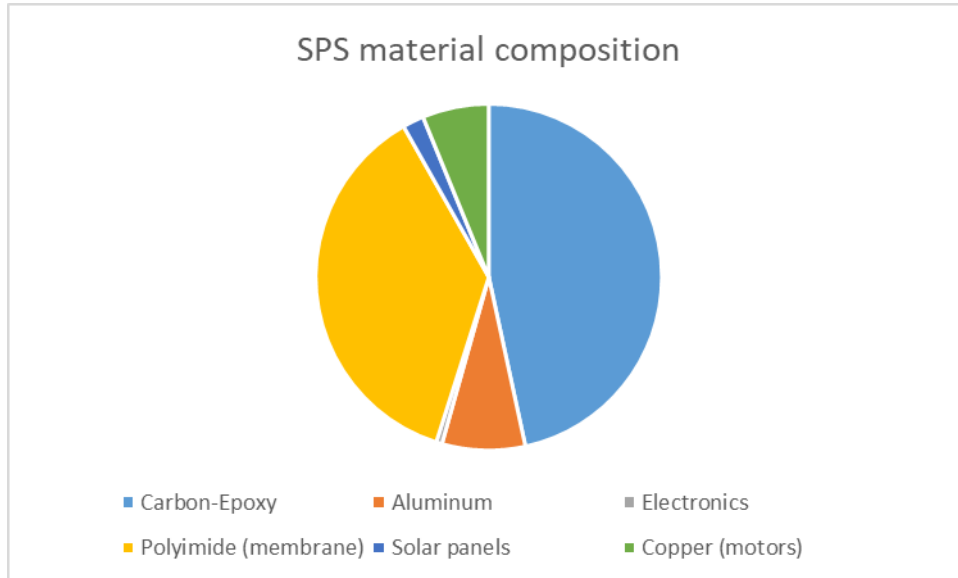
The table below shows a preliminary mass budget of the reflector.

Subsystem	Item	Quantity	Mass [kg]
AOCS	CMG rotor	2	650
	CGM support and suspension	2	1 000
	Secondary actuator (service module)	1	1 000
Structure	Structure	1	3 503
	Dual sided reflecting membrane	1	3 178
Communication	Omni-antenna + cables + support	2	2
	Transceiver	2	5
Power	Battery	3	5
	Solar arrays	1	255
	Power management	2	15
Data handling	Computer	2	10
	Sensors (3 STR, 2 IMU)	2	10
	Set of monitoring sensors	1	30
		TOTAL	11 365

Notices:

- If the membrane was fibre-reinforced, the additional mass would be 1600 kg to this total.
- It does not consider any margin for spare parts that could be hosted by the reflector.

The figure below shows the SPS material composition.



SRS material composition

4.2 Power budget

The table below shows a preliminary power budget of the reflector.

Subsystem	Item	Quantity	Power consumption [W]
AOCS	CMG	2	100
	Secondary actuator (service module)	1	8
Communication	Transceiver	1	5
Data handling	Computer	1	30
	Set of sensors (3 STR, 2 IMU)	1	10
	Set of monitoring sensors	1	30
TOTAL			283

4.3 Reference architecture synthesis

Orbit	Altitude	809 km
	Inclination	98.98 deg
	Orbit type	Sun-Synchronous, with repeating ground track
	Passes / cycle	14 orbits per 24h cycle
	Serviceable SPF	Up to 10 per orbit (every 4000 km)
	Number of reflectors	3987
Attitude control	Main actuator	2 x Control Momentum Gyros on the central mast, on each side of the membrane
	Rotor angular momentum	5105000 Nms
	Peak torque (total)	47000 Nm
	Rotor radius	10 m
	Rotor angular velocity	157 rad/s (1500 tr/min)
	Rotor material	Carbon fiber - Resin
	Secondary actuator	Centre of mass positioning wrt. drag and solar radiation pressure forces
	Total actuators mass	CMGs 3300 kg + Mobile mass 1000 kg
Structure	Type	Collapsed deployable triangular sections trusses of 1.16 m long
	Number of triangle sections for the ring	2700: 90 units of collapsed triangular sections of 35 m long
	Total single reflector mass (with actuators)	11 365 kg
	Size	1 km diameter circular rim with 540 m high central mast
	Areal density	14.5 g/m ²
	Material	Carbon fiber - Resin for structure, PEEK for membrane

5 Launch and assembly sequence

5.1 Launch solution

As already explained in [TN3] and detailed in part 2, DSR SBSP implies a very large number of reflectors: up to 3987 in the latest estimation.

It was assessed that a single reflector mass should be of about 11 t for an injection in SSO. Assuming Ariane 6 EVO and a new generation of European heavy fully reusable launcher injection mass in LEO SSO of respectively 17 t and 70 t, it could lead to respectively 2 592 and 630 launches if it was possible to split reflectors in multiple elements to optimize perfectly the launcher payload. But this latter solution implies an orbital assembly of these elements and doing so additional spacecraft as described in the part below.

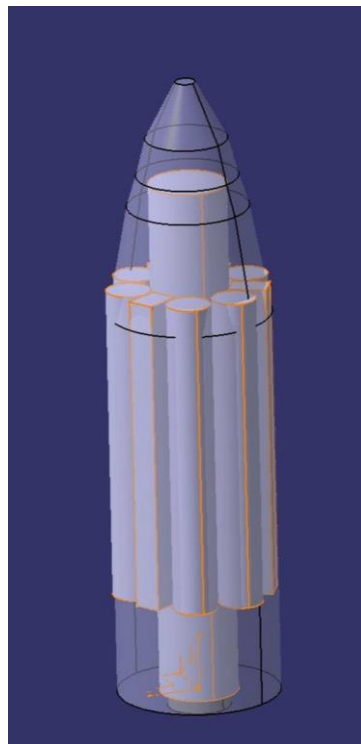


Figure 5-1: Folded reflector in A64 fairing

It is estimated that 3 reflectors kits could fit into the next generation launchers Starship and Protein fairings. It was also assessed for Protein an overall launch cadence of a launch every 3 days thanks to multiple launch pads and sites.

5.2 Assembly sequence

The figure below illustrates the assembly sequence of a launch batch of reflectors.

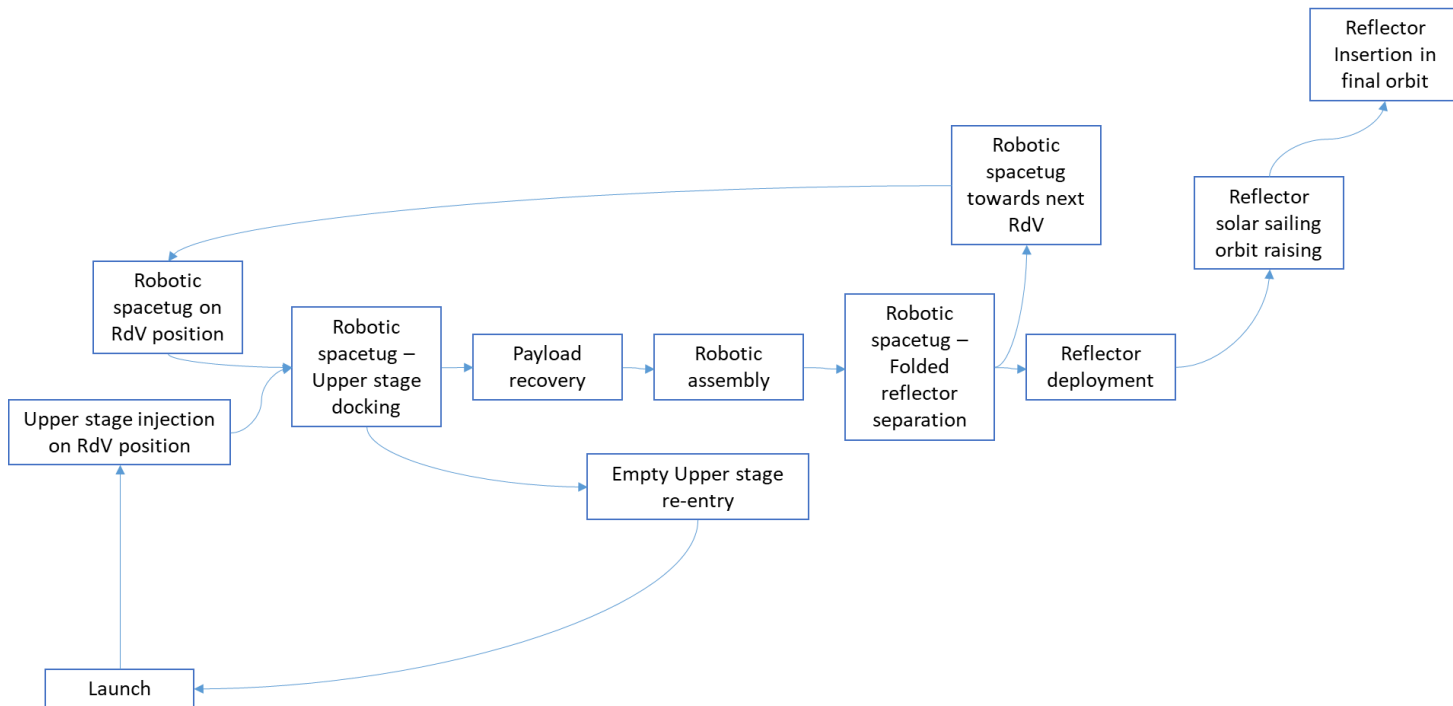


Figure 5-2: Reflectors logistics orbital assembly sequence

Launch

The launch time and injection accuracy are critical to avoid to postpone the rendezvous to the next opportunity.

Upper stage injection on RdV position

The launcher injects the Upper stage and its payload on a specific parking orbit where the Robotic spacetug is waiting for it. The Upper stage is in charge of the orbital phasing manoeuvres in absolute navigation.

Robotic spacetug – Upper stage docking

Robotic spacetug performs closing approach in relative navigation up to the docking. The Upper stage shall remain steady in attitude control while Robotic spacetug manoeuvres in order to dock to it.

Payload recovery

Once docked, the robotic spacetug, if need be, refuels itself from upper stage's tanks and proceeds with the payload extraction. The payload consist in a cluster of 3 reflectors elements organized to optimize both the fairing volume and the assembly sequence.

Empty Upper stage separation and re-entry

Once the payload cluster recovered by the robotic spacetug, the Upper stage performs a de-orbiting manoeuvre. If demisable it will perform a controlled re-entry and burn in the atmosphere. If it is reusable, it will be recovered and refurbished for another launch.

Robotic assembly

The robot of the spacetug proceed to reflector kit assembly by picking up elements of the payload cluster and building the reflector one piece at a time. This is a 4 day full time robotic work for the assembly of a single reflector.

Robotic spacetug – Folded reflector separation

Once the reflector assembly is complete, the Robotic spacetug proceed to reflector separation by pushing it at the maximum robotic arm reach and by using its thrusters to get distance between the spacecraft. Indeed, it is preferred not to perform the reflector deployment when it is still docked to the spacetug (and the other potential reflector kits) to avoid attitude and orbital disturbances due to the large structure.

Reflector deployment

Once separated, the reflector starts its deployment sequence which will probably take a few tens of hours to deploy the structure and the reflecting membrane. Then it starts its attitude control systems. In case of problem, the Robotic spacetug is still near and could perform reflector recovery.

Robotic spacetug towards next RdV

Once all of the reflectors kit assembled and dropped, the Robotic spacetug can move towards its next rendezvous zone. This motion is not necessarily based on costly manoeuvres but can be a combination of manoeuvres and long drift periods.

Reflector solar sailing orbit raising

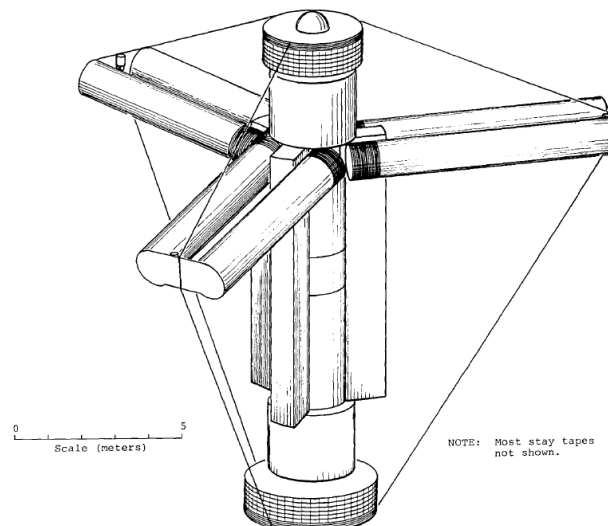
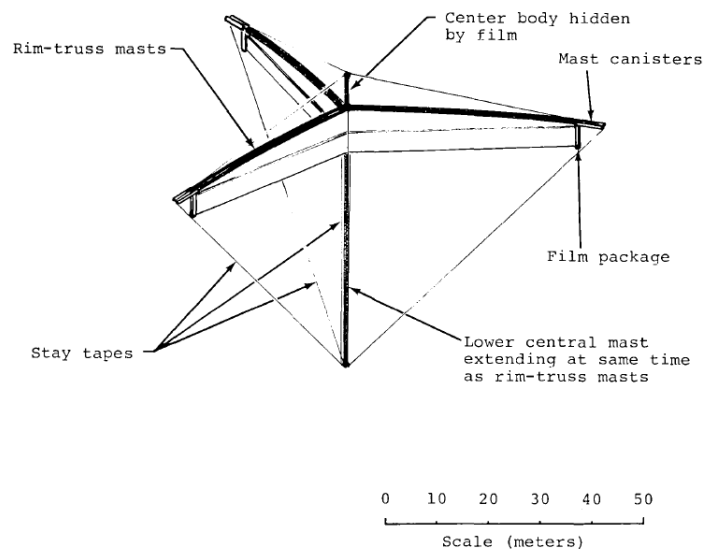
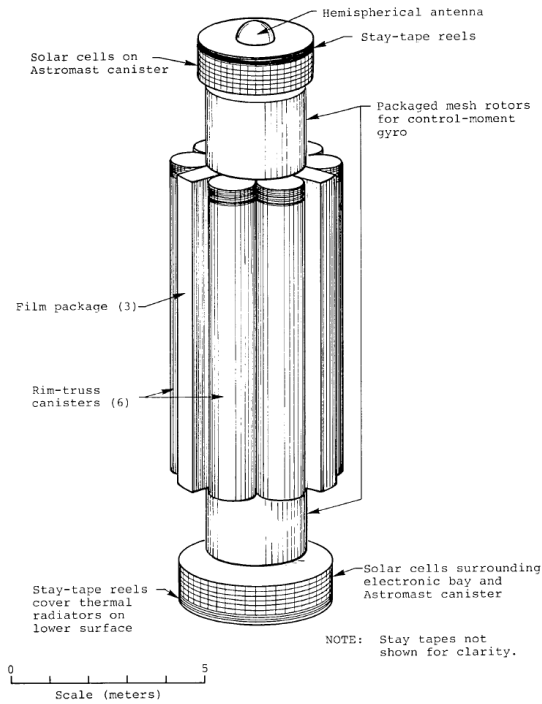
Immediately after its deployment, the reflector performs attitude control to orientate the reflecting surface to provide thrust for a solar sail orbit raising.

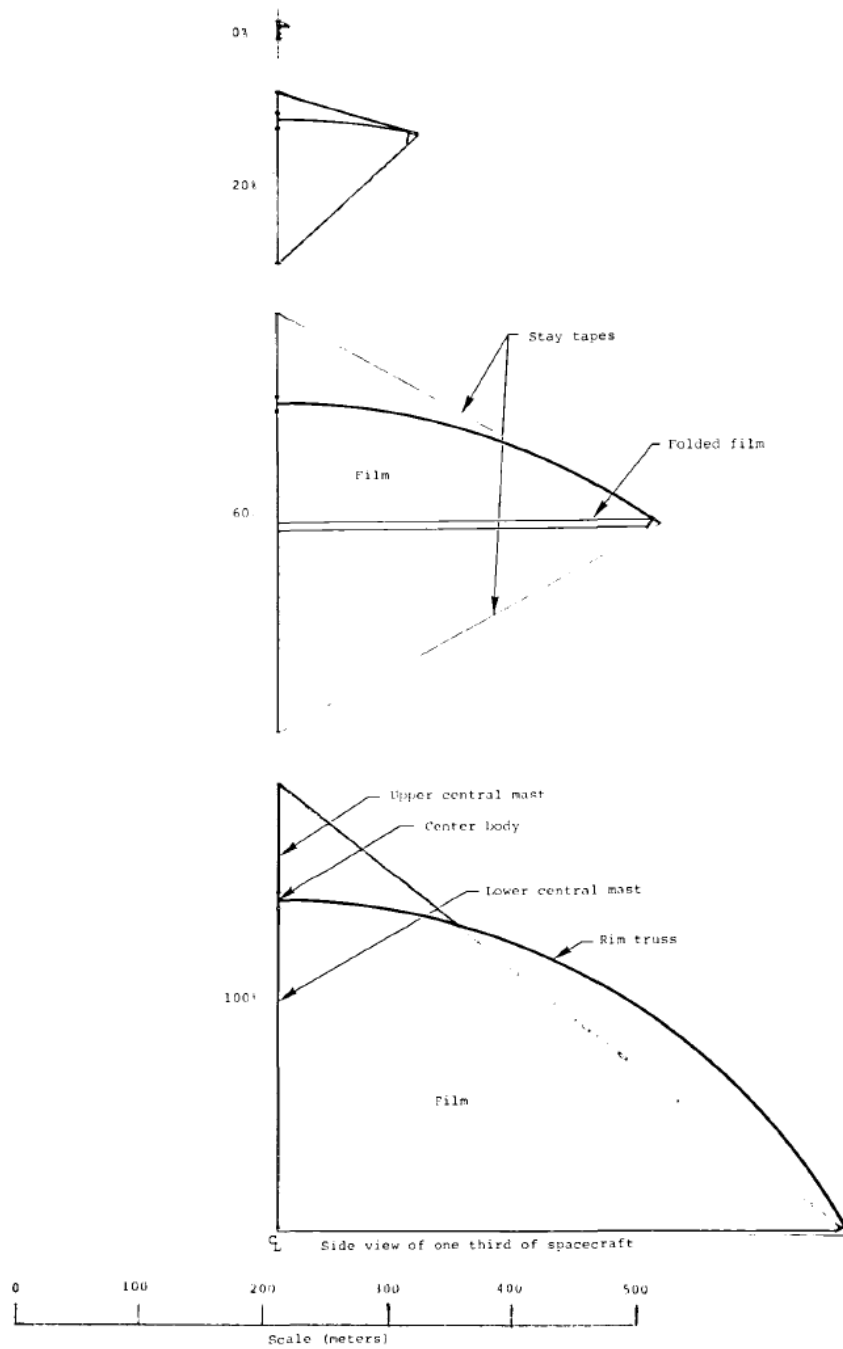
Reflector Insertion in final orbit

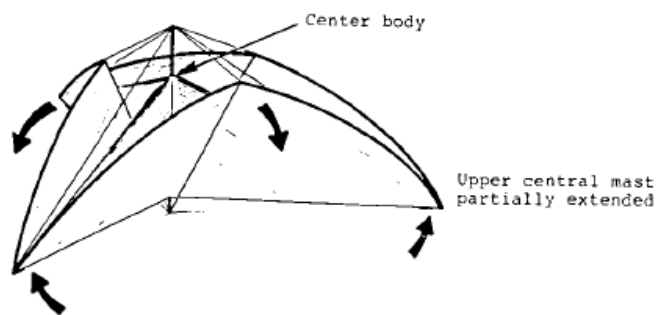
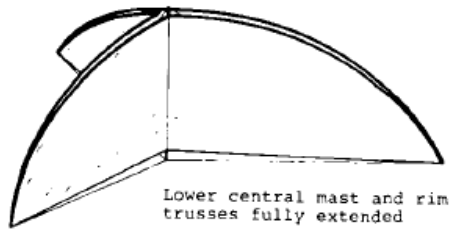
Once final orbit has been reached, the reflector shall orientate the solar sail thrust in order to insert itself in the reflector train position. This is a very critical manoeuvre because reflectors are only 12 km away from each other. The best is to add new reflector at the head or tail of the train to avoid complex insertions.

Target	3987 reflectors / 8 years		1,37 reflector/day	
Logistic node	Capability	Solution		
Launch cadence Protein	1 launch / 3 days 3 reflectors kit /launch	4 launch sites. Spec perf: 10 000 t/year LEO 6°.	1 reflector/day	
Launch cadence Starship	1 launch/8 days 3 reflectors kit /launch	Complementary Starship launches: 46 launches/year	0,38 reflector/day	
Orbital Assembly	1 reflector / robot / 4 days	8 hours to RdV with the launcher's upper stage 2 space trucks with 3 assembly robots each All robots working in parallel to deal with launch cadence	1,38 reflector/day	
Constellation building duration with current solution			7 years	11 months

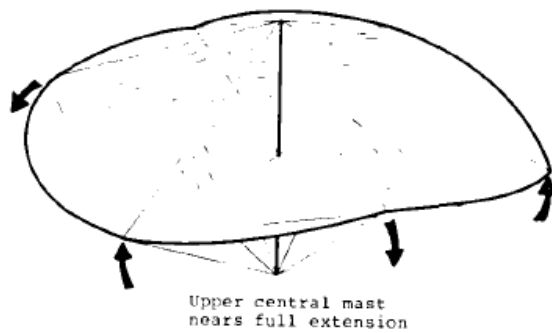
The figures below show the deployment sequence of NASA project. In our case, once the kit has been assembled by the robotic arm, the folded reflector will be very similar to the one illustrated below at the beginning of the sequence and will deploy autonomously after separation from the spacetug. The only noticeable difference between the two concepts is the CMG which is a solid flywheel of carbon-epoxy in our case assembled by robotic arm where it was a deployable filamentary CMG on NASA project.







NOTE: Most stay tapes not shown.



0 500
Scale (meters)

Film and rim fully deployed in final configuration



Figure 5-3: Reflector deployment sequence of NASA concept. Credits NASA [NASA]

6 Safety and end-of-life

A preliminary risk analysis has been provided in [TN2] and remain valid. However in this part we will discuss specifically the collision risk with space debris and micrometeoroids for which analyses have been performed during this study in order to evaluate it probability and effects.

6.1 Collision risk with debris and micrometeoroids

Such large platforms raise the question of collision risk with space debris and meteoroids. However, one can assume that in the next decade, the improvements in Space Situational Awareness will allow to detect any object above 1 cm and issue a warning message with a very thin uncertainty thanks to space surveillance sensors and orbit propagators improvements. It could then reasonably reduce the uncertainty of the collision point on the reflector to a few tens meter square large area. At that point, the collision risk could be managed according to a combination of multiple strategies:

- “Let it be”: by estimating that given the debris energy and the probable zone of collision, it is acceptable to let the collision happen,
- Perform an attitude correction to minimize/nil the collision risk or its potential damages,
- Perform an orbital correction manoeuvre to minimize/nil the collision risk or its potential damages,

Thanks to SRS attitude control system, its ability to reorient the platform in order to present a low profile to reduce significantly or nil the collision risk is very fast, and is estimated to about 5 minutes maximum thanks to AOCS sizing. This is a very short time with respect to the expected period of time available to react from the early collision alert received tens of hours before. This makes these attitude avoidance manoeuvres the favoured ones because they minimize the impact on the nominal operations.

For the collisions that could not be avoided by an attitude manoeuvre, an orbital avoidance manoeuvre is then necessary. It is estimated that this manoeuvre could be performed using solar sail / drag force propulsion if started soon enough, which should be the case because we are here talking about detectable and tracked objects for which the alert is typically received several days before the collision. As an example, given the mass of the platform and with a worse case of atmosphere density (only $6.15e-16$ kg/m³ according to NASA atmosphere model) applying a solar / drag sailing profile during 4h could lead to a miss distance of about 250 m with drag effect only (solar radiation pressure contribution not considered here). Practically, it means that only a few hours of mission interruption to proceed to orbital avoidance manoeuvre, adopting a special solar/drag sail profile, should be necessary for the SRS before to recover its nominal pointing pattern.

However for smaller debris and meteoroids that elude any detection mean, we performed a statistical analysis thanks to DRAMA tool to evaluate if they are of concern.

Because DRAMA is not designed for such large surface (limited to 1000 m²), we made the following hypotheses:

- Reflecting membrane was considered separately as it is not a structural element
- All the other “solid” unitary structural elements made of cylindrical trusses of 15 mm diameter and 1 m long were compacted in order to create a continuous volume of which we considered the orientation presenting the highest cross-section surface. This 277 m² surface was used for a 10 year propagation run (DRAMA cannot propagate further).

The results details are in annex but they show a probability of collision of 100% with objects of up to 2.5 mm after 10 years, and no collision risk with objects bigger than 7 mm.

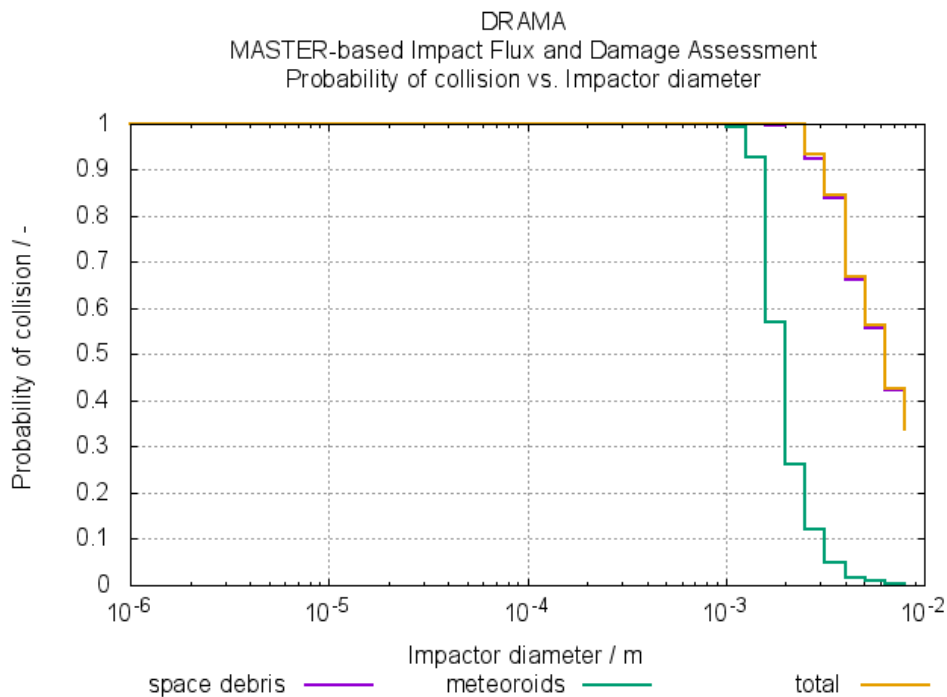


Figure 6-1: DRAMA results over 10 years, structure only

This analysis also predicts about 70 collisions with debris or micrometeoroids of 1 mm, and up to 700 collisions for debris slightly smaller (0.7 mm) over 10 years.

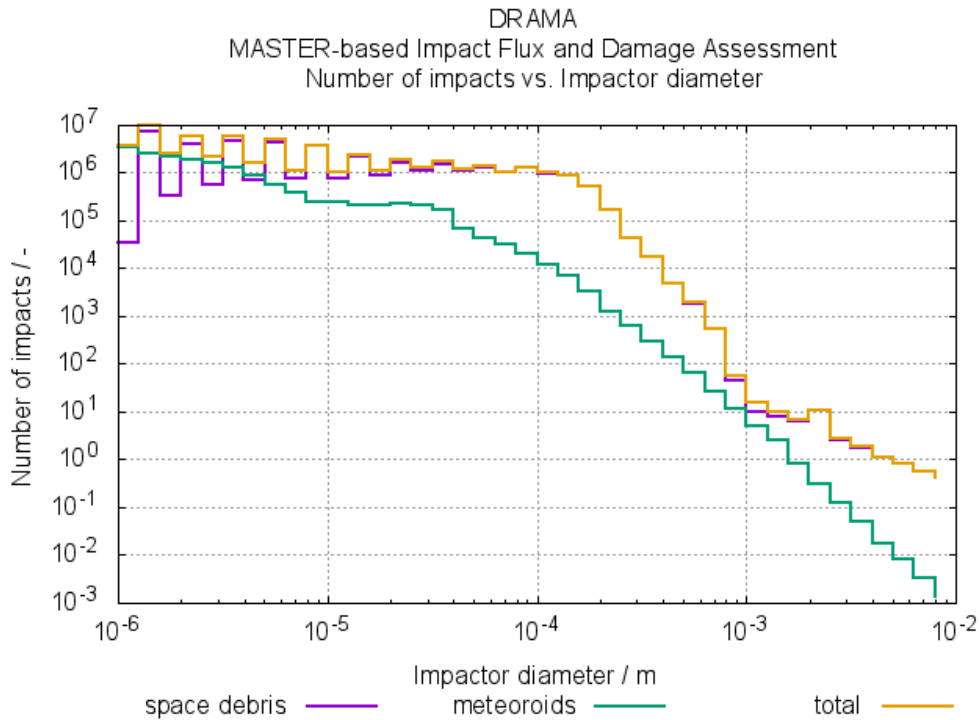


Figure 6-2: DRAMA results over 10 years, structure only

This is a real concern because even if involving small particles striking elementary beams, which compose most of the platform structure, these collisions should not be considered as catastrophic but they should certainly lead to an immediate reflector rotation interruption to stop structural constraints and to allow the inspection and repair operations. If such measures have to be taken for each impact, it would lead to a poor system availability and robotic repair systems on each reflector, with a large number of spare parts.

The figure below illustrates very well the effects that could have the impacts mentioned in the statistics above as they deal with the same materials characteristics and debris size.

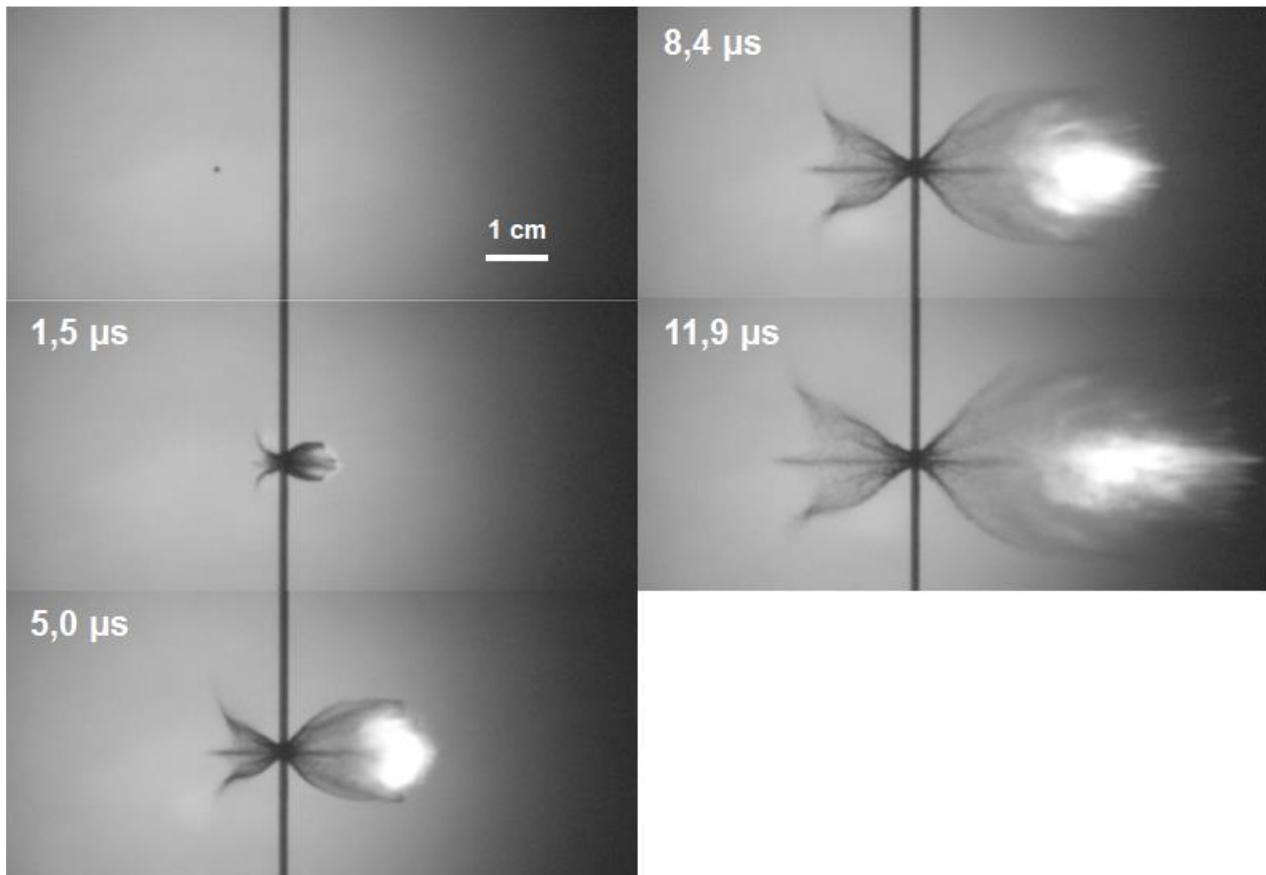


Figure 6-3: Fast imaging of a 1 mm Al6061 bullet impacting a 400 µm thin carbon fiber-epoxy target at 5.62 km/s and resulting debris cloud. Vincent Jaulin thesis tel-03641686 ENSTA Bretagne

For instance, no measure to deal with these small particles collision risk is proposed except to strengthen the beams, increasing the platform mass, or to assessing deeper the collision risk and the impacts consequences on the structural elements.

The following figure shows the growth of the number of impacts along the next decade.

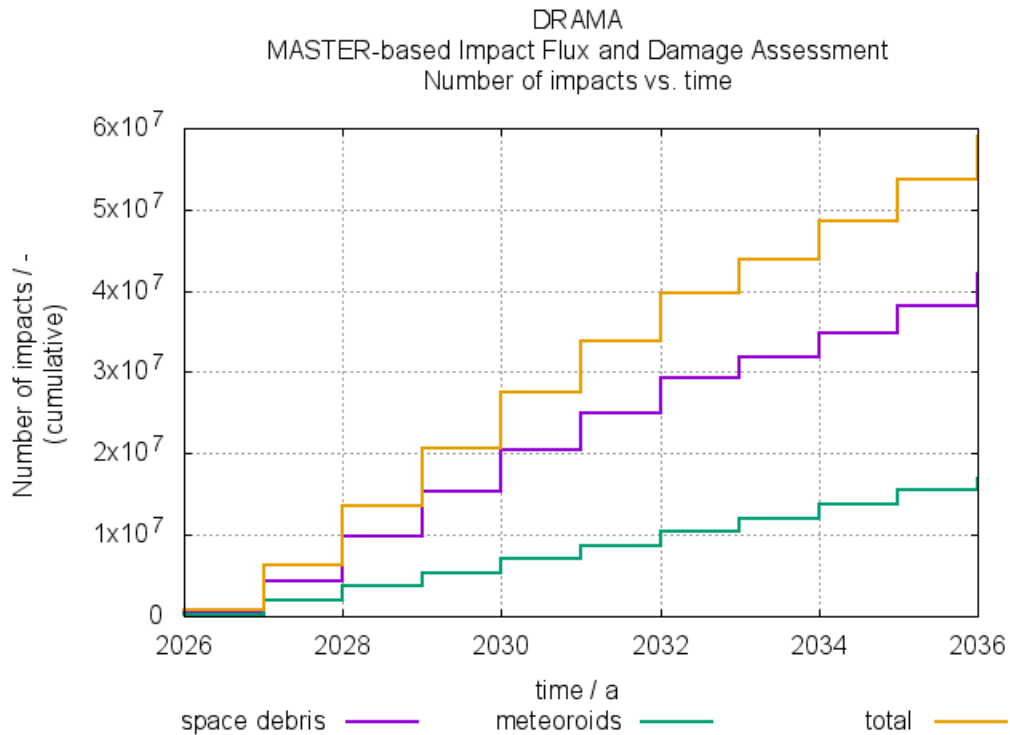


Figure 6-4: DRAMA results over 10 years, structure only

For the membrane, because of the DRAMA limitation, the computation was run for a surface of 1 000 m² and then the following results should be multiplied by 785 to get the cumulative number of impacts leading to penetration, i.e. piercing the membrane.

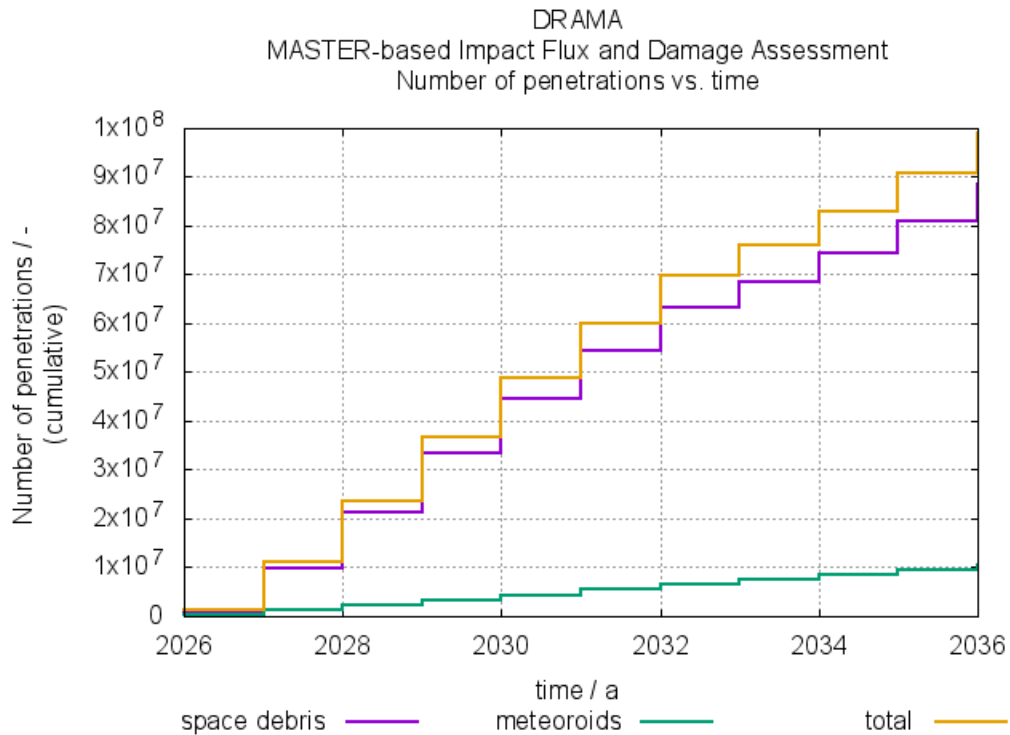


Figure 6-5: DRAMA cumulated penetration impacts

For a 1 km diameter membrane, it makes a cumulated number of 74.6 billion impacts, i.e. an average of 9.5 penetrating impacts per cm² after 10 years. It is then reasonable to plan a membrane replacement to compensate the membrane erosion due to impacts with debris.

As an example, the potential solution to double the thickness (and mass) of the membrane would divide the number of penetrating impacts by about 1.4.

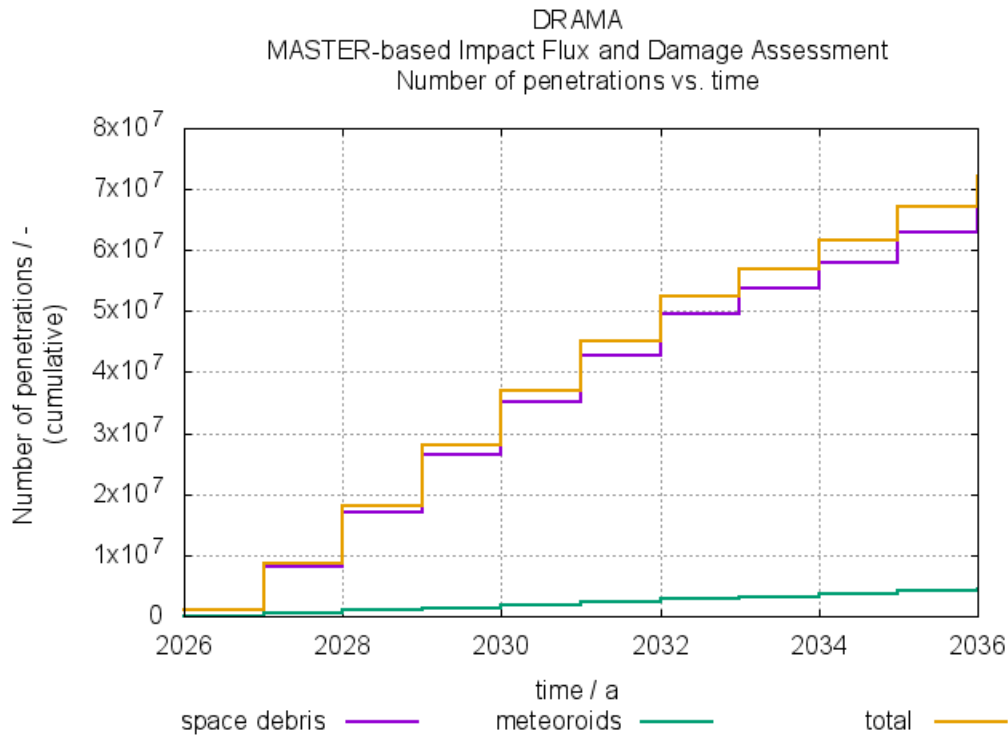


Figure 6-6: Number of cumulated penetrating impacts if the membrane was 8 µm thick.

We see then that to increase the thickness alone is not necessarily the best solution. Finally the problem with debris on the membrane is not so the alteration of the reflecting capacity because cumulated holes will represent only a few percent of loss over 30 years. The real concern is to tear the membrane due to weaknesses induced by holes. To prevent from that risk, a solution could be to combine a thin fibre material like Optiveil® inside a PEEK reflective membrane. This would increase the overall mass and thickness of the membrane, probably by 50%, but should ensure the needed tear resistance over the mission.

MATERIAL COMPOSITION

Description:	Wet-laid nonwoven fine E glass fibre veil
Fibre Type:	Fine E Glass
Fibre Length:	12 mm / 0.5"
Fibre Diameter:	6 µm
Binder Type:	PVA (poly vinyl alcohol)

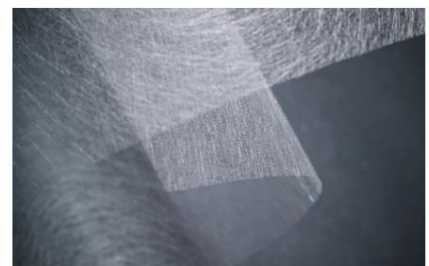


Figure 6-7: Optiveil® nonwovens thin layer. Credits Technical Fibre Products Ltd

Such a fibre reinforcement of the membrane should ensure tear resistance to both micro abrasion due to micro particles impact, but also tear resistance of holes induced by larger debris. For the latter, the size of the largest debris manageable is not linked to the fibre length as the role of the fibres is not to prevent from a hole to appear but to prevent from a tear to propagate. Given the relative collision speed and the membrane material and thickness, it is considered that membrane's surface in contact with the debris will immediately be vaporized, leaving a neat hole thanks to fibre reinforcement. Therefore the maximum manageable impact size on the membrane is more dependent to the repair capability provided by servicing robots acting on the surface of the platform and their ability to deploy a patch. This could be a sizeable patch soldered onto the membrane (PEEK material allows soldering). As we assumed that debris of 10 cm and larger could be avoided, collisions with smaller debris perpendicular to the surface of the membrane should not generate holes larger than the debris itself. In the same way, in case of non-perpendicular collisions, the ellipsoidal shape of the hole should not have a minor axis larger than the hole. In this latter case, the patch would consist in a stipe of membrane appropriately sized.

However, this estimation shall be taken with care because first the almost 4000 1 km reflectors will share these collisions and moreover it is very likely that they will "sweep" the orbit, reducing the debris population crossing this orbit (of course not applicable to micrometeoroids). Indeed, collisions will generate new debris, but they will be smaller with much less energy. Finally very small debris of a few microns will vanish, vaporized in a plasma after collision. DRAMA simulations do not take these particular effects into account so it is not yet possible to assess more precisely the collision risk on the membrane and the effect of large numbers of large surface structures over the mission lifetime.

6.2 Collision risk with satellites

It was also assessed how crowded is the selected orbit (SSO at 890 km), first to figure out if populating this orbit with 4000 large reflectors is just possible and also to have an idea of the future collision avoidance operations.

The table below synthesizes the filtering results obtained from the US Space-Track.org database fed by US Space Command.

Orbital envelope considered	Nb. sat
Same orbit (SSO, altitude +/-10km & local time +/-1h)	0
SSO, altitude (+/-10km), not same local time	6
Altitude (+/-30km)	24
Altitude (+/-40km)	132

Number of satellites today present in the considered envelope. Source: Space-Track.org database

The results show that today, there is no known satellite nearing the same orbit as SRS train in an envelope of +/-10 km and +/-1h local time of the SSO). Relaxing the filtering criteria to consider any local time SSO for this same altitude envelope only leads to 6 satellites.

Now relaxing even more the criteria to any kind of orbits (not only SSO) to an altitude envelope of +/-30km, only contains 24 satellites.

Finally, it is only when considering an altitude of +/-40km that the number of satellites populating this envelope becomes to increase to up to 132.

As a result, it can be considered that as of today the selected orbit is not too crowded for the deployment of the reflectors' train because there is no satellite using exactly the same orbit and only a few of them that could potentially cross the orbital train in the neighbourhood, finally inducing a limited number of collision avoidance operations with satellites. However this is a first order of magnitude of the situation, as elliptical satellites and launchers' upper stages drifting with respect to the selected orbit should also be considered in a thorough analysis during the demonstration phase.

6.3 Other risks

6.3.1 Radiation

There is no particular critical sensitivity of the SPS with respect to radiations, essentially because SPS system do not rely on an electronics payload like for observation or telecom satellites. So a redundant set of flight proven avionics is considered enough to perform the mission.

The other point with the radiation is the material alteration, particularly of concern for the reflective membrane. For it, no specific assessment has been made because the material selected are already flight proven and qualified for at least 20 years.

6.3.2 Space weather events

The main risk due to space weather is the atmosphere dilatation due to Sun peak of activity. Even if at an altitude of 890 km this was not initially assessed as a problem, it will be necessary in a next study to estimate if the solar sailing station keeping is still possible during these periods.

6.4 FDIR and critical events

The table below is an update of the one provided for ASR. It also add the information of severity and likelihood.

		Severity		
		High	Medium	Low
Likelihood	High			
	Medium			
	Low			

Risk	Risk nature	Risk assessment		Detection	Effect	Measures
		Severity	Likelihood			
Collision with space debris	Collision	High	Low	Alert from Space Situational Awareness organization	Reflector damage. From minor to critical. Generation of debris.	Size the critical elements of the platform accordingly, protect with a shield. Use next generation of space debris tracking. Perform orbital and/attitude manoeuvres for collision avoidance Replace reflector by a spare reflector
Collision with micro space debris (not indexed in catalog)	Collision	Low	High	Structural sensors (strain gauges, shock detectors), camera inspection.	Reflectors alteration. Depending on the impact energy and location	Size the critical elements of the platform accordingly, protect with a shield and pray
Collision with micrometeoroids	Collision	Low	High	Structural sensors (strain gauges, shock detectors), camera inspection.	Reflectors alteration. Depending on the impact energy and location	Size the critical elements of the platform accordingly, protect with a shield and pray
Collision with other reflectors of the fleet	Collision	High	Low	Flight dynamics collision alert	Reflectors destruction	Design of the constellation with enough distance between reflectors to let time to react. Accurate and permanent relative orbital control
Loss of attitude control	Fault	Low	Low	Sensors and TM and ground monitoring	Beam hazardous orientation on Earth	Beam interruption system. Attitude recovery program. Space servicer intervention. Limit the max power beam of a unit reflector
Reflector hacking	Attack	High	Low	From abnormal behaviour to a sudden total loss of control	From abnormal behaviour to a sudden total loss of control	Satellite crypto protection and monitoring software Limit the max power beam of a unit reflector
Satellite too bright	Fault	Low	Medium	From modeling at conception. From ground visual observations after launch.	Environmental disturbance	Design of the platform (geometry, material) limiting unexpected reflecting surfaces. Attitude control to avoid to direct the beam towards Earth when not on a PV farm.
Major solar storm	Environment	Low	Medium	Avionics and communications anomaly	Avionics damage. Up to reflector control loss.	Size the avionics to survive major solar storms. Space servicer spacecraft assistance for attitude and orbit recovery and repare.
Deployment failure of large pre-manufactured structures	Operations	High	Medium	Sensors and TM and ground monitoring. In situ robotic monitoring.	From temporary deployment failure up to reflector loss.	Multiple versatile robots helping in the deployment and fixing problems

Preliminary FDIR list

6.5 De-risking approach with demonstration

The demonstrator is the first step to further study key points of the infrastructure to derisk the main issues linked with DSR performance

Main considerations for the DSR system related to risks to be assessed during the SSD phase

ConOps	Questioning	Solutions under consideration to be further analyzed	Actions planned during the demonstrator phase
Launch & Deployment			
Assembly	<ul style="list-style-type: none"> Can SRS be deployed autonomously ? 	<ul style="list-style-type: none"> Use the NASA design 	<ul style="list-style-type: none"> Full simulation + test of the first SRS launched
Attitude control & Maintenance	<ul style="list-style-type: none"> Can the structure withstand the proposed rotation rates? 	<ul style="list-style-type: none"> Structure composed of two control systems: CMGs and secondary actuators with a mass 	<ul style="list-style-type: none"> Detailed analysis Full simulation
Attitude control & Maintenance	<ul style="list-style-type: none"> What is the control strategy for a flexible structure? 	<ul style="list-style-type: none"> Implementation of a control system for flexible structure: SSD will be representative of the structure's flexibility 	<ul style="list-style-type: none"> Detailed analysis Full simulation Test on the first SRS launched
Attitude control & Maintenance	<ul style="list-style-type: none"> How do vibrations caused by CMG will impact the structure dynamics? 	<ul style="list-style-type: none"> Flywheel is projected to be perfectly balanced to avoid any vibrations 	<ul style="list-style-type: none"> Detailed analysis Test in labo
Attitude control & Maintenance	<ul style="list-style-type: none"> Where will be positioned the counterweight on the structure? How will its movements affect the spacecraft ? 	<ul style="list-style-type: none"> The moving mass could in fact move in 3D, on most of the locations of the structure (rim, mast and spokes) The motion of the counterweight is slow and essentially translations along the spokes and mast and its objective is to lighten the torques that CMG has to manage 	<ul style="list-style-type: none"> Detailed analysis Full simulation Test in labo Test on the first SRS launched
Collision risk management	<ul style="list-style-type: none"> How will impacts deform the membrane? 	<ul style="list-style-type: none"> PEEK material has been selected to avoid any extensive thrown of the membrane. The membrane is kept flat by peripheral tension 	<ul style="list-style-type: none"> Full simulation Test in labo Test on the first SRS launched
Collision risk management	<ul style="list-style-type: none"> How can the structure be reinforced to limit the debris creation? 	<ul style="list-style-type: none"> Several options are considered to improve the membrane resistance: adding a layer of graphene absorbing debris, thinner and more rigid beams to reduce the surface exposed 	<ul style="list-style-type: none"> Detailed analysis Full simulation Test on the first SRS launched
End of life	<ul style="list-style-type: none"> What is the best end-of-life policy for each component of the SRS? Considering the re-entry on Earth, could we ensure that the debris does not have an energy >15J? 	<ul style="list-style-type: none"> Natural orbit decay and burn in atmosphere Return to Earth by solar sail or with space tug Return on parking orbit and recycling (on longer-term) 	<ul style="list-style-type: none"> Detailed analysis Full simulation

6.6 End of life management

Different possible strategies for end of life should be combined to avoid any new debris

- No end of life, maintained forever.** This solution seems obvious: can't we exploit SBSP for much more than 30 years after so many energy spent to make it work? The cost for that is to maintain in operational conditions the system. However it is not really satisfying as one day or another a new power production will certainly be more efficient than SBSP, like nuclear fusion.
- Design for recycling/refurbishing.** In this approach, the space segment is designed to be recycled or refurbished in space. Used parts can be dismantled and stored in a space warehouse waiting for recycling. The recycling space factory could use solar power to melt, separate and transform materials, for example in a centrifugal solar furnace. Design for recycling supposes that the space segment uses only recyclable materials in its conception and its architecture will ease the dismantling process.
- Decommissioning and place in a graveyard orbit.** This is a classical approach in which after operational life, the spacecraft is placed, by itself or thanks to a space tug, to an orbit on which it could not interfere with current or future mission. The definition of graveyard orbits is subject to change and it is hard to anticipate what could still be allowed in several decades.
- Dismantling and cargo return to Earth.** This approach consists in dismantling the space infrastructures and take them back on Earth in the cargo bay of reusable upper stages which otherwise would have returned empty. It implies a considerable spent of energy but this is the cost for a much more virtuous space usage than simply burning things in the atmosphere.
- Natural orbit decay and burn in atmosphere.** This is also a today practice but it is not sure to be still allowed in the future due to sanitary reasons (in cause the small particles spread in the atmosphere during re-entry burn). However this solution is simple for large and lightweight platforms like reflectors for which the drag force acts significantly in LEO.

► Recycling, orbit decay and controlled return on earth are the main actions to avoid any additional debris

The approach is to focus on orbit decay before the recycling/ refurbishing capabilities

End of Life per component in space

Component	Policy	Rationale	Risk
Mirror	When not reusable, orbit decay Recycling the material could be interesting to limit the replacement of reflector	Large flat with very low density	Low
Beam	1/ Can be reused for new DSR 2/ Controlled re-entry on Earth	Relative low density but solid with potential long lifetime	Low
Service module	1/ Change electronic card (plug & play) 2/ If not, orbit decay	Small service module that could be reused with new electronic cards	Low
Robot	Controlled re-entry on Earth	Avoid any new debris	Low
Tug & platform	Controlled re-entry on Earth	Avoid any new debris	Low
Fuel tank	Controlled re-entry on Earth	After refueling, the tank can use the return trip of a launcher	Low

Comments

- The two most pragmatic solutions are:
 - The orbit decay and burn in atmosphere**
Components such as the mirror and most part of the beams will return by solar foil to a lower orbit, and then be disintegrated
 - The controlled re-entry on Earth**
This approach is chosen for components such as the robot, tug or fuel tank which will not burn in atmosphere
- On the long term, **design for recycling/refurbishing** is the most promising policy as it avoids any waste.
 - It will allow to **maintain the structure in orbit** and a **deployment of recycling system** will be implemented in orbit
 - However, the **TRL is still very low** and it cannot be the selected policy, even if it could be the best one

- ▶ The material that could be used for component will be selected to offer the best compromise cost/ sustainability/ possibility with orbit decay

Regarding the design for recycling approach, it was not considered in the frame of this study because its low TRL and of the lower mass efficiency with respect to the proposed architecture in which the structure is in carbon epoxy. However, it is interesting to note that the structure could be composed of inflatable structures made of PEEK, like the membrane. This material can be easily recycled on Earth today and one can imagine that thanks to an orbital recycling station based on a centrifugal solar furnace, most of the SRS material could be recycled, becoming a resource for future orbital projects. This orbital resource would be so much more affordable since already in space, with no more launch cost.

7 Technology maturation needs and small scale demonstration

This preliminary study allowed to identify the technology gaps or uncertainties to be consolidated. In this part we propose to address them in a roadmap illustrating what could be the next steps paving the way towards space based solar power.

Phase 0/A/B1 study

Main objectives: analyse further the SBSP concept and propose a sub-scale space based demonstrator

In this activity:

Take time to complete the LEO Direct Solar Reflection vs. GEO Solar Pumped Laser trade-off to the light of the pre-phase A outcomes (current study) that spotted, post ASR, unforeseen technical difficulties in the DSR concept.

Propose a detailed concept of operations and preliminary mission analysis

- Define the optimal launch strategy
- Detail the SBSP ecosystem operations and elaborate delta-V budget for each component
- Demonstrate the constraints concept of formation flying with solar sail

Modelling of the AOCS and structural design in order to assess the slew and pointing performance. This is a crucial point as the reflector agility drives the number GPS that could be fed by the reflectors and so impacts directly the business model.

- Evaluate the resulting mechanical loads on structure and CMGs actuators during the mission.
- Evaluate the pointing performance of the beam and resulting spot shape and irradiance.
- Evaluate in detail the solar sailing orbit raising strategy

Reflecting membrane design

- Evaluate the possibility to manage dynamical membrane shape for stabilization, beam control and potentially focusing
- Select the reflector membrane material, thickness and tension system

Elaborate an optimized reflector architecture in order to be dismantled in kit for launch, then assembled in orbit by robotics means and then deployed autonomously.

- Identification and modelling of mechanical elements and
- Splitting/folding of the platform in kit elements

Analyse the space environment effects on the reflector, and particularly radiation and thermal effects on electronics, membrane and structure fatigue and collision risk and effects from micrometeoroids and debris. For debris collision an analysis of the generation of new debris vs. sweep effect should also be performed.

Propose a demonstration plan for which the steps could be:

- CONOPS and mission analysis of the demonstration
- Ground demonstrations when possible,
 - Simulation modelling of the system: mission analysis, AOCS, formation flying, mechanical, thermal
 - Structural mechanical testing
 - Zero-G demonstration with ground support equipment for structure deployment
 - If need be, Zero-G parabolic flights
- Subscale space demonstrator
 - 100 – 1000 m² mechanically representative sub-scale reflector platform
 - Autonomous deployment in space
 - Orbit raising Solar sailing
 - CMGs attitude control
 - Membrane impacts collision detection and analysis
- Minimum Viable Product: to initiate the business with a subscale reflector (potentially the same as the previous

8 Annexes

8.1 DRAMA analysis report

Cf. dedicated pdf.

8.2 Natural frequencies of the platform.

We look for the frequency of vibration of assembly composed of

- the mirror PEEK plane (4 μ m, density = 1.3 kg/L),
- the circonferencial carbon rim-truss and
- the carbon truss mast.

Mast is linked to rim-truss by stiff (carbon) 90 links; and to membrane at its middle.

The frequency would be found using the (Rayleigh)-RITZ method, where the displacement is decomposed into a pondered sum $a_n(t)$ of basis functions $f_n(x,y,z)$; where the a_n coefficients are determined through a system of n linear equations; these equations being obtained by minimizing the energy of deformation of the displacement.

Before undertaking this compute, we need to understand the relative comportment of each part of the system, taken as if isolated: we mean to find

- the frequency of the membrane alone;
- the frequencies of the rim-truss;
- the frequency of the mast.

This will increase our insight in the relative "speed" of each of these 3 elements.

The membrane frequency (see ref ..Timoshenko¹ and ref .. Rayleigh²): according to surfacic mass; the first frequency of interest for the membrane is **0.019 Hz**.

For a circular membrane of radius "a"; unit surfacic mass "rho" , under tension " T", simply supported at it's circumference,

¹ Timoshenko « vibration problems in engineering » 2nd ed 1937. § 68

² Rayleigh « theory of sound. Vol 1" 1877. § 200.

the first mode frequency is

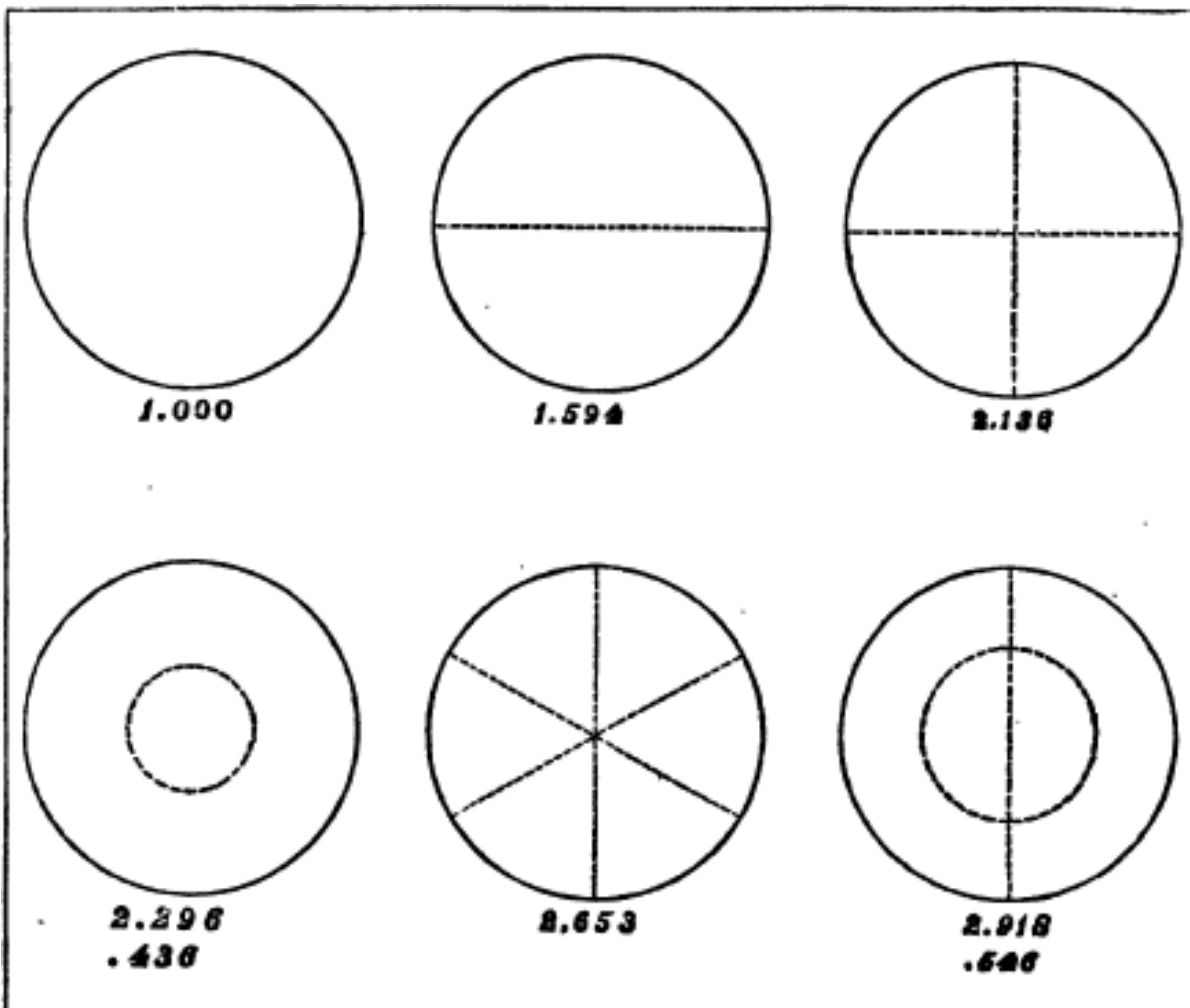
$$f_0 = 1 / (2\pi) \cdot 2.404 \cdot 1/a \cdot [T/\rho]^{0.5}$$

in our case (T=1.2 N/m; rho = 4.9E-3 kg/m²; a=500 m); we have

$$f_0 = .012 \text{ Hz.}$$

For higher modes of the membranes, the frequencies, and there associated mode shape are illustrated here-below (from ref RAYLEIGH); where we retained of specific interest the case where a diametral line is nodal (counted from up_left to down_right in the figure, there are cases n°2; n°3; n°5; n°6).

(the first figure is the ratio of the frequency of the mode to the one of the first mode (which is our f₀); the second figure (when present), is the ratio of the radial nodale circle (when present) to the membrane diameter.



Translated in our membranes, this results in the following table:

case	Freq = f ₀ *	Freq [Hz] for f ₀ =0.0118 [Hz]

N°2	1.59	.0189
N°3	2.136	.0253
N°5	2.653	.0315
N°6	2.918	.0347

Further cases are referenced in ref Timoshenko; we use the table in ref Timoshenko with “s” the number of radial nodes and “n” the number of angular nodes; and divide some values in the first 3 lines by 2.404 (the reference coefficient of the ref); which illustrates the ratio of the modes frequency to the fundamental.

s	n = 0	n = 1	n = 2	n = 3	n = 4	n = 5
1	2.404	3.832	5.135	6.379	7.586	8.780
2	5.520	7.016	8.417	9.760	11.064	12.339
3	8.654	10.173	11.620	13.017	14.373	15.700
4	11.792	13.323	14.796	16.224	17.616	18.982
5	14.931	16.470	17.960	19.410	20.827	22.220
6	18.071	19.616	21.117	22.583	24.018	25.431
7	21.212	22.760	24.270	25.749	27.200	28.628
8	24.353	25.903	27.421	28.909	30.371	31.813

2.404	1	1.59400998	2.13602329	2.65349418	3.15557404
	2.29617304	2.91846922	3.38893511	4.02246256	
	3.59983361	4.16638935			

Our conclusion is that for the case of interest, the first frequency of the membrane (case n° 2) will be at around 0.019 Hz.

The Rim-truss frequency : first mode transverse to plane at **0.03 Hz**

(the truss is considered free, without the membrane)

The ref .. Timoshenko gives, for “flexural vibrations involving displacement at right angle to the plane of the ring (and twist) the frequencies of the principal modes are

$$.f_n = 1/(2 \pi) [E I / (\rho A r^4) n^2 (n^2 - 1)^2 / (n^1 + 1 + \nu)]^{0.5}$$

Where A the area of cross section and “v” is the poisson ratio ³

We obtain :

n	2	3	4	5
.fn [Hz]	0.0295	0.085	0.16	0.26

Comparing the rim-truss deformations and the membrane deformation in the different modes of both ; we find that rim-truss frequencies are significantly higher than membrane “corresponding” frequencies; except for the first mode, where rim-truss frequency is not so far than for the following modes, but nonetheless at a frequency 55% higher than “corresponding” membrane frequency.

Rim-truss mode	Membrane mode n°	Rim-truss freq	Membrane freq
2	2	0.0295	0.0191
4	3	0.16	0.026

Mast frequency : a first frequency at **0.17 Hz**

Considering the mast as a beam of young modulus 2.E11 , area 0.00016 m2 ; distance (of longeron) to the beam center 1.06 m ; linear mass rho 0.2777 kg/m ; we find a reference frequency

$$.fref = 1/(2\pi) \beta^2 [EI / (\rho A)]^{0.5}$$

Which gives

$$.fref = 140 \beta^2 \text{ kHz}$$

Where β is determined by the boundary condition; for pinned-pinned at both extremities and L at 270 [m]; $\beta = \pi/L$; which gives a first bending at

$$.fo = 0.17 \text{ [Hz]}.$$

(Considering the axial compression of the beam at 622N, a small correction put the frequency at 6% lower than fo; the corrective factor being evaluated at $(1 - [\text{compression_load}/(\pi^2 EI / L^4)]^2)$).

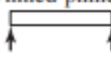
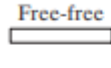
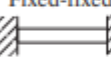
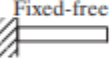
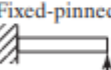
From ref RAO⁴ :

Lateral vibration of the mast is evaluated as:

³ (note that for flexural displacement in-plane of the ring, the frequencies are very similar, and obtained putting as if “v” equal zero in precedent expression).

⁴ RAO mechanical vibration. Ed 6th. 2001

$$\omega = \beta^2 \sqrt{\frac{EI}{\rho A}} = (\beta l)^2 \sqrt{\frac{EI}{\rho A l^4}} \quad (8.93)$$

End Conditions of Beam	Frequency Equation	Mode Shape (Normal Function)	Value of $\beta_n l$
 Pinned-pinned	$\sin \beta_n l = 0$	$W_n(x) = C_n [\sin \beta_n x]$	$\beta_1 l = \pi$ $\beta_2 l = 2\pi$ $\beta_3 l = 3\pi$ $\beta_4 l = 4\pi$
 Free-free	$\cos \beta_n l \cdot \cosh \beta_n l = 1$	$W_n(x) = C_n [\sin \beta_n x + \sinh \beta_n x + \alpha_n (\cos \beta_n x + \cosh \beta_n x)]$ where $\alpha_n = \left(\frac{\sin \beta_n l - \sinh \beta_n l}{\cosh \beta_n l - \cos \beta_n l} \right)$	$\beta_1 l = 4.730041$ $\beta_2 l = 7.853205$ $\beta_3 l = 10.995608$ $\beta_4 l = 14.137165$ ($\beta l = 0$ for rigid-body mode)
 Fixed-fixed	$\cos \beta_n l \cdot \cosh \beta_n l = 1$	$W_n(x) = C_n [\sinh \beta_n x - \sin \beta_n x + \alpha_n (\cosh \beta_n x - \cos \beta_n x)]$ where $\alpha_n = \left(\frac{\sinh \beta_n l - \sin \beta_n l}{\cos \beta_n l - \cosh \beta_n l} \right)$	$\beta_1 l = 4.730041$ $\beta_2 l = 7.853205$ $\beta_3 l = 10.995608$ $\beta_4 l = 14.137165$
 Fixed-free	$\cos \beta_n l \cdot \cosh \beta_n l = -1$	$W_n(x) = C_n [\sin \beta_n x - \sinh \beta_n x - \alpha_n (\cos \beta_n x - \cosh \beta_n x)]$ where $\alpha_n = \left(\frac{\sin \beta_n l + \sinh \beta_n l}{\cos \beta_n l + \cosh \beta_n l} \right)$	$\beta_1 l = 1.875104$ $\beta_2 l = 4.694091$ $\beta_3 l = 7.854757$ $\beta_4 l = 10.995541$
 Fixed-pinned	$\tan \beta_n l - \tanh \beta_n l = 0$	$W_n(x) = C_n [\sin \beta_n x - \sinh \beta_n x + \alpha_n (\cosh \beta_n x - \cos \beta_n x)]$ where $\alpha_n = \left(\frac{\sin \beta_n l - \sinh \beta_n l}{\cos \beta_n l - \cosh \beta_n l} \right)$	$\beta_1 l = 3.926602$ $\beta_2 l = 7.068583$ $\beta_3 l = 10.210176$ $\beta_4 l = 13.351768$
 Pinned-free	$\tan \beta_n l - \tanh \beta_n l = 0$	$W_n(x) = C_n [\sin \beta_n x + \alpha_n \sinh \beta_n x]$ where $\alpha_n = \left(\frac{\sin \beta_n l}{\sinh \beta_n l} \right)$	$\beta_1 l = 3.926602$ $\beta_2 l = 7.068583$ $\beta_3 l = 10.210176$ $\beta_4 l = 13.351768$ ($\beta l = 0$ for rigid-body mode)

(we consider the case pinned-pinned for the half-mast , of 270 m length).

Including rotations (along center-line) will reduce the frequency of the mode, but not significantly with respect to the conclusion regarding the total assembly; which is object of the next paragraph:

Total assembly:

Clearly, the mast is very stiff.

We conclude that the lowest frequency mode is the one where the mast holds the rim-truss; and the membrane vibrates as if in the free mode referred "mode n°2" (in §membrane), which is at 0.019 Hz.

This freq is proportional to square root of the ratio "tension / surfacic_mass" of the membrane.

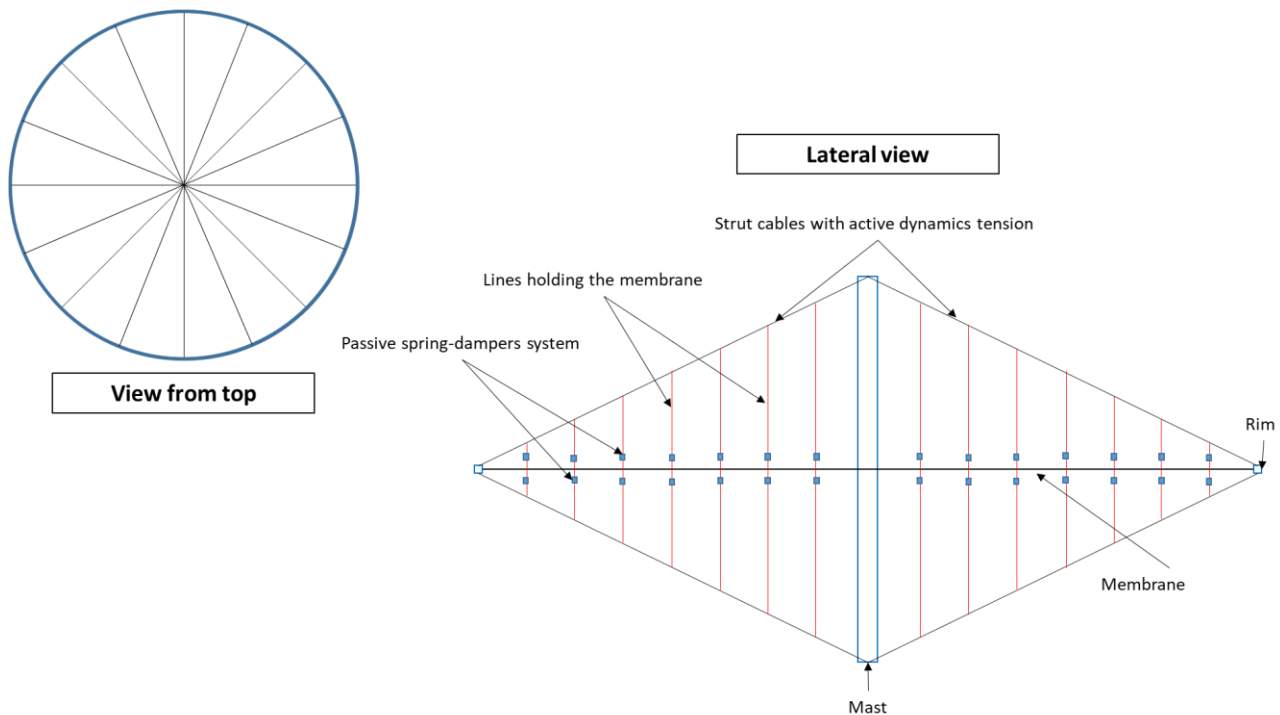
Possible solutions to manage

It is important to highlight that several solutions could be combined to deal with this low natural frequency to make possible attitude control of this large structure, particularly to reach the pointing performance.

First, since the lowest frequency comes from the membrane, two solutions can be considered:

1. To make the membrane lighter by selecting a 2 μm thin membrane. Even if such a thickness seems reachable today, the counterpart is that it is less resistant to tears and space debris/meteoroids impacts.
2. To damp the membrane oscillations with lines connecting the membrane to spokes. Indeed, the simple fact to add these connections increases noticeably the frequency of the membrane's natural modes. In addition, use of dampers and springs along these lines could then deal with the residual oscillations.

The second is preferred since it saves mass and is very efficient. Indeed if used in as illustrated in the figure below, it would shift the natural frequency from 0.019 up to 0.18 Hz.



Platform solutions to deal with membrane low natural frequency

In complement to the previous solution, an active control of the spokes cables tension to dampen the oscillations of the structure can be used to compensate membrane and structure oscillations.

And last but not least, elaborate a smart attitude control law able to deal with pointing performance while preventing from natural modes excitation. It would be a very complex control law given the number of sensors (strain gauges, optical/laser metrology, ...) and actuators (passive: dampers, active: CMGs and screw jacks for the lines) involved in the loop but this complexity can be managed with nowadays simulation tools.

End of document